Stress Relaxation in Poly(methyl methacrylate) (PMMA)

At Large Strains During The Process Of Hot Embossing

THESIS

Presented in Partial Fulfillment of the Requirements for Graduation with Distinction, Bachelor of Science at The Ohio State University

By

Akul Kakumani

Undergraduate Program in Mechanical Engineering

The Ohio State University

2013

Defense Committee:

"Dr. Rebecca Dupaix, Advisor"

"Dr. Carlos Castro"

Abstract

Poly(methyl methacrylate) is a strong and lightweight polymer which has a number of applications, hot embossing being one of them. The output of an embossing process, a surface profile, involves monitoring a number of factors such as strain rate, total strain, embossing temperature and spring back. Due to its glass transition of around 107˚C, PMMA is an ideal candidate for this process and is used in multiple manufacturing techniques. Previous experimental work in this area had led to the development of a mechanical model which inaccurately predicted stress relaxation in the polymer at higher temperatures. The purpose of this project was to improve this model by performing experiments incorporating certain factors that were not included before, such as cooling the sample and spring back. For this, a number of samples were tested at temperatures above their glass transition temperature using an Instron testing machine. The samples were compressed between two compression plates, and held at a constant strain level for a specific period of time. During this period, the stress in the material was recorded by measuring the force exerted by the sample on the compression plate. Similar tests were carried out by varying the test parameters and the differences in stress relaxation behavior were observed. At the end of a test, spring back in the sample was recorded after a period of one hour. Percent spring back was calculated based on these values, and along with data obtained from the experiments, was incorporated in the mechanical model. Simulations from this mechanical model were compared with the experimental data and it was found that this model fits the new stress relaxation with cooling data reasonably well. By further improving this mechanical model, PMMA's behavior under complex loading conditions can be determined which will ultimately reduce trial and error in the mold design procedure, and benefit the industry by saving time and money.

To my family and my grandfather for supporting me all the way since the beginning of my studies

To Ohio State, my home away from home

Acknowledgments

I would like to express my deepest appreciation to my advisor, Dr. Rebecca Dupaix, for her continued support and encouragement: she continually and convincingly conveyed a spirit of adventure with regards to research, and an excitement with regards to teaching. Without her guidance and persistent help this thesis would not have been possible. I'm indebted to Dr. Castro for taking time out of his busy schedule and being on my Defense Committee.

I would like to thank my group member, Danielle Mathiesen, for proving support academically and inspiring me with her commitment to the highest standards. I'm most grateful to Peng He for helping me out with my experiments despite his academic commitments.

A special thanks to my friend Akshay Jain for assisting me with my simulations. In addition, I would like to thank my friend, Nicholas Bons, for introducing me to areas to which my project could be branched out to.

Last, but by no means least, I thank all those people who shared their technical expertise in the field of machining and helped start this project.

Vita

March 2008…… FIITJEE Junior College

Sept. 2008- March 2011……..B.S. Civil Engineering, Osmania University

March 2011-Present……....B.S. Mechanical Engineering, The Ohio State University

Fields of Study

Major Field: Mechanical Engineering

Table of Contents

List of Tables

List of Figures

CHAPTER 1

Project Background

Poly(methyl methacrylate) (PMMA) is a synthetic polymer of methyl methacrylate and is often used as a lightweight or shatter-resistant alternative to glass owing to its moderate properties, easy handling and processing, and low cost (1). The presence of the pendant methyl (CH_3) groups prevents the polymer chains from packing closely in crystalline fashion and from rotating freely around the carbon-carbon bonds. As a result, PMMA is a tough and rigid plastic. In addition, it is an ideal substitute for glass as it has an almost perfect transmission of visible light, and retains these properties over years of exposure to ultraviolet light and weather. Also, as PMMA displays the unusual property of keeping a beam of light reflected within its surfaces, it is frequently made into optical fibers for telecommunication or endoscopy (6).

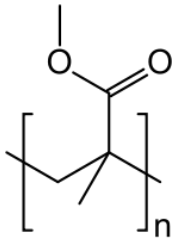

Figure 1: PMMA (Cavette, n.d.)

Furthermore, because of the above mentioned properties, PMMA is used for a wide range of applications such as hot embossing, room temperature imprinting, injection molding, laser ablation, in situ polymerization and solvent etching (2). Hot embossing is the process of stamping a pattern into a polymer softened by raising the temperature of the polymer just above its glass transition temperature. The stamp used to define the pattern in the polymer can be made in a variety of ways including micromachining from silicon, LIGA, and machining using a CNC tool, the latter used primarily for making large features. A wide variety of polymers have been successfully hot embossed with micron as well as nano sized features, including polycarbonate and PMMA. This technique is primarily used for defining micro-channels for fluidic devices. The benefits of this approach are the ability to take advantage of the wide range of properties of polymers, as well as the potential to economically mass produce parts with micron-scale features. (7) Hot embossing is especially well suited for manufacturing small and medium-volume series, because the mold insert can be exchanged within a rather short period of time. Another advantage is the discrete material supply. In this way, polymers can be changed from one molding cycle to the next without any hardware modification being required(8). Hence it is important to determine the right combination of parameters to improve this process by making it much more efficient. Considering the germaneness of PMMA, it is important to dwell further into the subject of this polymer so as to better exploit it for these applications.

One defining aspect of a polymer is its glass transition temperature, the temperature at which it transitions from a solid state to a more viscous state. Compression tests are being customarily performed to obtain an accurate model of PMMA near its

glass transition temperature, 107°C, or for that matter any polymer. Earlier tests performed by D. Vogtmann involved testing a specific number of PMMA samples within an environmental chamber that had been heated to PMMA's glass transition temperature. The samples, placed between two plates, were compressed at a constant rate and then held at a constant compression level for a specific time period known as the holding period. During this period, the stress in the material is recorded by taking into consideration the force applied by the sample on the plates. Several tests were conducted by varying the temperature, compression rate and compression level during the holding period. Based on the changes in the loading conditions and the temperature, the differences in the stress relaxation behavior of PMMA were observed. These differences were examined through several data manipulation techniques as well as comparing the results with a viscoelastic stress relaxation model.

An example of the data that was captured and plotted is shown below:

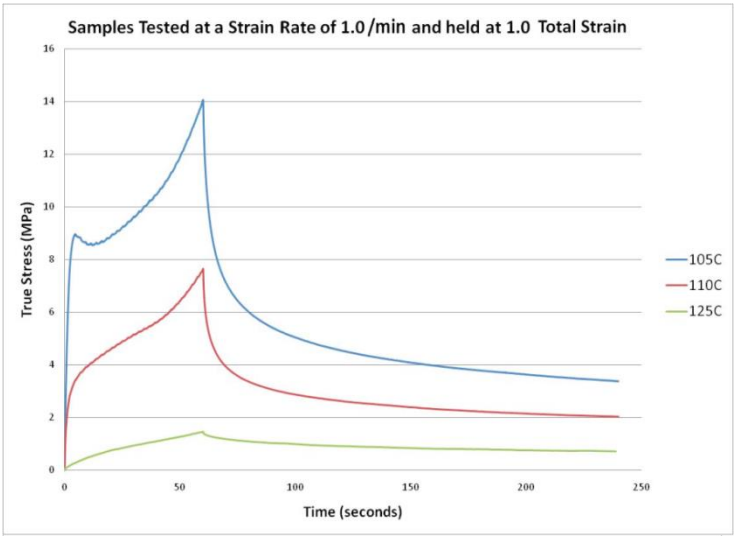

Figure 2: Strain rate 1.0/min, Total Strain 1.0 at different temperatures (Vogtmann, 2009)

This figure shows true stress plotted against time at different temperatures above PMMA's T_g. In a similar way, a variety of graphs involving the test parameters were plotted to study the notion of stress relaxation. Finally these results were compared with simulations from a mechanical model, Maxwell in this case, and based on these comparisons the model was further enhanced. Building off of these, the experimental procedure was further enhanced in the current project and an analogous procedure was pursued to develop a mechanical model.

Figure 3 shows a comparison made by D. Vogtmann between data obtained from an experiment and a simulation using Maxwell model. This model, even though it resembles PMMA's behavior quite accurately for the later part of the curve, doesn't bode well for the initial part.

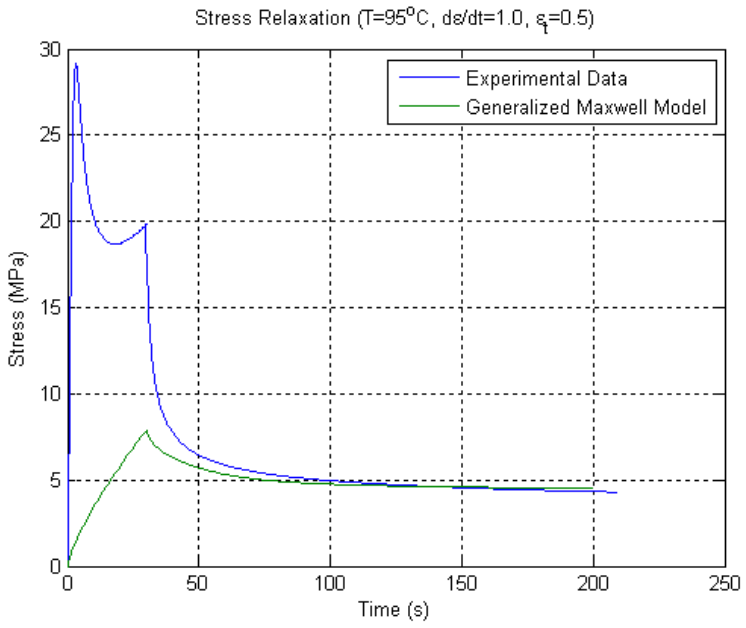

Figure 3: Maxwell Model Simulation with ramp input (Vogtmann, 2009)

These mechanical models make use of parallel and series combinations of linear and non-linear springs and dampers. The equations defining these springs and dampers are achieved by analyzing and simulating data obtained from the compression tests and assigning a curve fit to it. This model is expected to mirror a polymer's behavior at various temperatures under diverse loading conditions. Earlier models such as the Dupaix-Boyce model posed difficulties at temperatures farther above glass transition where PMMA has no clear yield point or strain hardening at high strains (3).

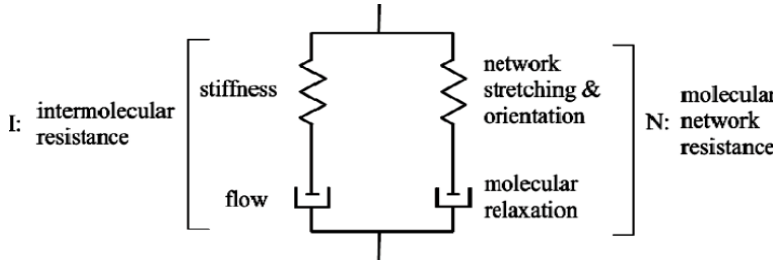

Figure 4: Schematic of Dupaix-Boyce model (Vogtmann, 2009)

In the model shown above, the deformation gradient in each branch is equal to the total deformation gradient, $F_I=F=F_{N,}$ whereas the total stress is equal to the sum of the Cauchy stress in each branch, $T_I+T_N=T$. Ghatak-Dupaix conducted further experiments to conclude that while the Dupaix-Boyce model worked for temperatures near the glass transition temperature, the fluids based Doi-Edwards model was a better fit for temperatures more than 15°C above the glass transition temperature. Ames, et al. (2009) further ameliorated this model by introducing a third branch in parallel to the two branches. Depending on whether the temperature is below or above the glass transition

temperature, the second or the third branch is activated in the model. The drawback to this model lies in the fact that it involves 50 material constants for the curve fit, thereby making simulations tedious (4).

Stress relaxation behavior in PMMA has been recorded for temperatures ranging from T_g-15°C to T_g+25°C using compression tests under varying conditions. The goal of this project is to capture the stress relaxation behavior of PMMA during compression while following a procedure pertaining to industry standards. This research will contribute to the broader research activities of Danielle Mathiesen and Dr. Dupaix of developing a material model for PMMA.

Objectives

Some of the main objectives of this research are to collect mechanical data for PMMA in embossing processing regime by varying temperature, true strain and strain rate. The sample is to be cooled after compressing and holding it for a specific period of time which in turn depends on the strain rate being used. The springback of the sample is measured after the end of the experiment. Finally, this data is interpreted and used to plot the necessary graphs detailing the stress relaxation behavior of PMMA under different loading conditions and varying temperatures. These plots are compared with the stress relaxation plots of data obtained previously when samples were tested without the introduction of a cooling system. These stress relaxation plots, the ones with cooling as well as the ones without, are compared with the existing mechanical model to determine any necessary changes that are to be made to the model for it to better represent PMMA's

stress relaxation behavior. These changes are made by tuning the variables governing the model behavior within a specific range of values.

Additionally, experiments are performed on PMMA substrates using hot embossing molds containing different micro-channel patterns. These tests are load controlled and after the embossing process, the micro-channels imprinted on the sample are observed under a microscope to determine their profiles.

The whole process has been divided into different chapters and discussed in detail below. Chapter 1 details the initial process and materials used for the experiments. The results obtained, which mainly consist of stress relaxation plots of PMMA under different loading conditions, have been listed in Chapter 2. Chapter 3 sees a comparison made between simulated data procured from the Mathiesen model and the experimental data while chapter 4 talks about the second phase of the project, the molding experiments. A brief description of the conclusions and future work in chapter 5 rounds up the developments.

These objectives have been met besides performing some compression testing simulations on PMMA in ANSYS.

CHAPTER 2

Equipment Used

The samples of PMMA used in the experiments had a height of 8.8 mm and a diameter of 10 mm. These samples were machined from a large sheet of acrylic that was supplied by Plaskolite, Inc.

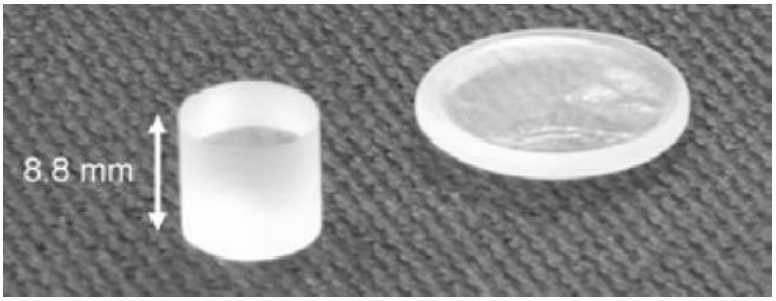

Figure 5: PMMA samples before (left) and after deformation (Vogtmann, 2009)

In order to compress the samples of PMMA, an Instron 5689 screw driven material testing system is used. It consists of an Instron 3119-409 environmental chamber with temperature control, a static lower plate and a movable upper plate whose displacement varies according to the test conditions. This arrangement is run by a software known as Instron Bluehill via an Instron 5800 controller. The software contains a profiler using which a strain profile is set up in the system to control the movement of the upper compression plate. The displacement of the compression plate along with the force exerted by the sample onto this compression plate is recorded by the software. This recorded data is used to calculate stress and to check whether the strain profile was

correctly input in the first place. A National Instruments USB-TC01 J-type 3 Thermocouple Probe 781314-03 is also used to obtain the temperature profile during the experiment.

Testing Procedure

The basic steps to run the experiment are listed below, with more elaboration on some of the specifics in the subsequent paragraphs.

For PMMA stress relaxation experiments:

1) Heat the environmental chamber with the compression plates to the desired experimental temperature for a period of two hours.

2) Load Bluehill software and use the profiler to define a procedure.

3) Place a thermocouple on top of the static compression plate in the environmental chamber and plug its other end containing a USB port to the computer.

4) Place a thin sheet of teflon, lubricated with WD-40, on each of the compression plates and place the sample between these sheets.

5) Hold the sample in the chamber for twenty minutes for it to reach the experimental temperature.

6) Lower the upper compression plate so as to have minimum contact with the sample.

7) Reset gauge length and balance load.

8) Run the program and start the stopclock. Note the time after which the desired true strain is reached and add three minutes to it. Call this time t_{cool}. After t_{cool}, open the door

of the chamber to cool the sample.

9) Wait for the program to end and stop the temperature logger. Save output data from the program.

The Profiler

The profiler allows the programmer to control the testing procedure by defining strain rate and true strain. Displacement of the force plate and the total time taken make up the basis of the independent profiles that constitute the profiler. Previous tests demonstrated that limiting the number of steps to 28 produced repeatable results. The total time required to reach the desired true strain at the desired strain rate is calculated and divided among 27 of these steps. To start with, the change in height for the first interval is determined and subtracted from the original height to get the new height, based off of which the displacement for the next interval is determined.

$$\Delta h = hi * \varepsilon$$
$$h_{i+1} = hi - \Delta h$$

Δh= Change in height

h_i= Height at the beginning of the interval

h_{i+1}= Height at the end of the interval

Following this method, the necessary displacements for subsequent intervals at the specified strain can be calculated. These 27 profiles together are known as the loading period while the 28^{th} interval, inputted with a constant strain level for a desired period of

time, is known as the holding period.

Depending on the parameters, Bluehill software can be programmed to output desired variables. A sample strain profile is shown below.

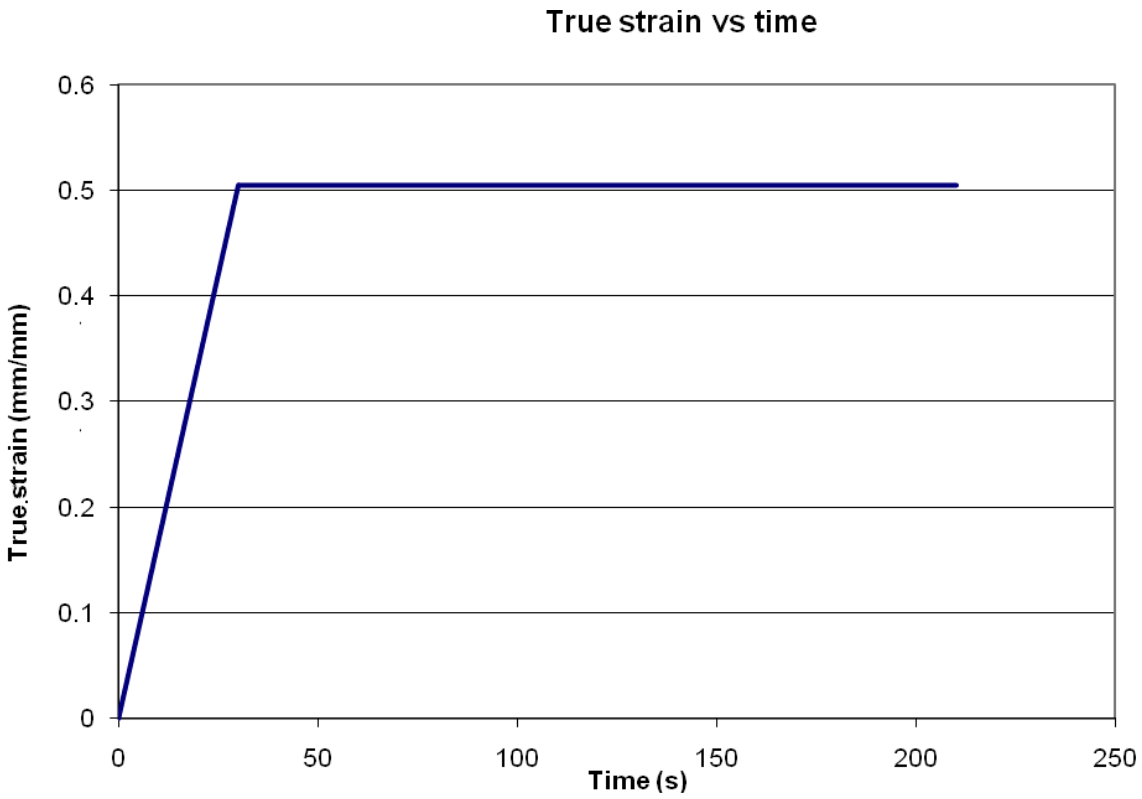

Figure 6: Strain profile

Sample Preparation

To start with, the desired testing profile is selected in the Bluehill software. After this, thin sheets of Teflon, lubricated with WD-40, are placed on the top and bottom compression plates, and the sample is placed between these sheets. Each sample, before being tested, is placed in the environmental chamber for a period of 20 minutes. This ensures that the sample uniformly attains the temperature of the chamber. A schematic of

the setup is shown below.

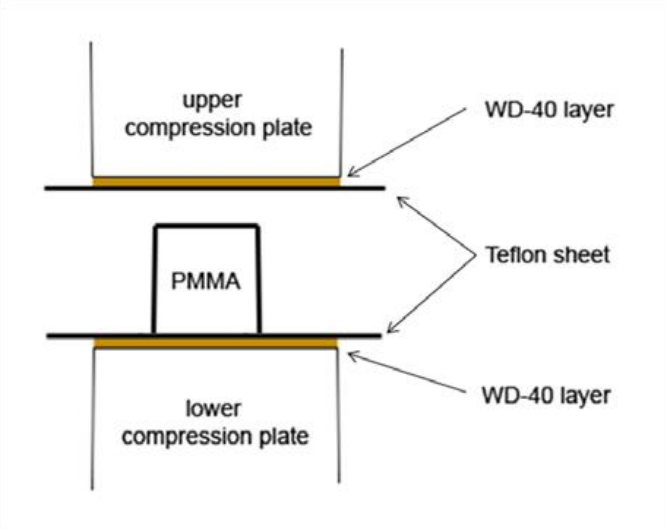

Figure 7: Experimental Setup

The Teflon sheets, along with WD-40, are used to allow the sample to expand laterally with minimum friction and to avoid direct contact between the sample and the lubricating material.

True Stress, Strain Rate and Temperature

Various combinations of true stress, strain rate and temperature were used to test the samples. The following test matrix details these combinations:

Table 1: Test matrix (blue portion=test combination)

Total Strain	Temperature							Strain Rate
	105°C	115°C	125°C	135°C	145°C	155°C	165°C	
0.5 ε								0.5 ε/min
1.0 ε								
1.5 ε								
0.5 ε								1.0 ε/min
1.0 ε								
1.5 ε								

The samples were tested at temperatures ranging from 105°C-135°C, at strain rates of 0.5 ε /min and 1 ε /min while varying the total strain between 0.5 ε and 1.5 ε. Some tests were also performed at elevated temperatures of 145°C-165°C to get an estimate of the temperature range defining the test procedure.

Repeatability

Two to three samples were tested for every combination of test parameters. This was done to ensure repeatability of the test results as well as to avoid sample deforming, seen in figure 8, which arose as a result of inappropriate test parameters. Samples were first tested for deformity and next for repeatability. If any of the above two criteria failed, the test parameters were altered and the samples tested again. Data obtained from tests run using the same parameters were close to one another, with deviations ranging from 0-5%. An example of the data obtained from tests conducted using the same parameters is shown below in figure 9.

Figure 8: Curling of sample upon unloading

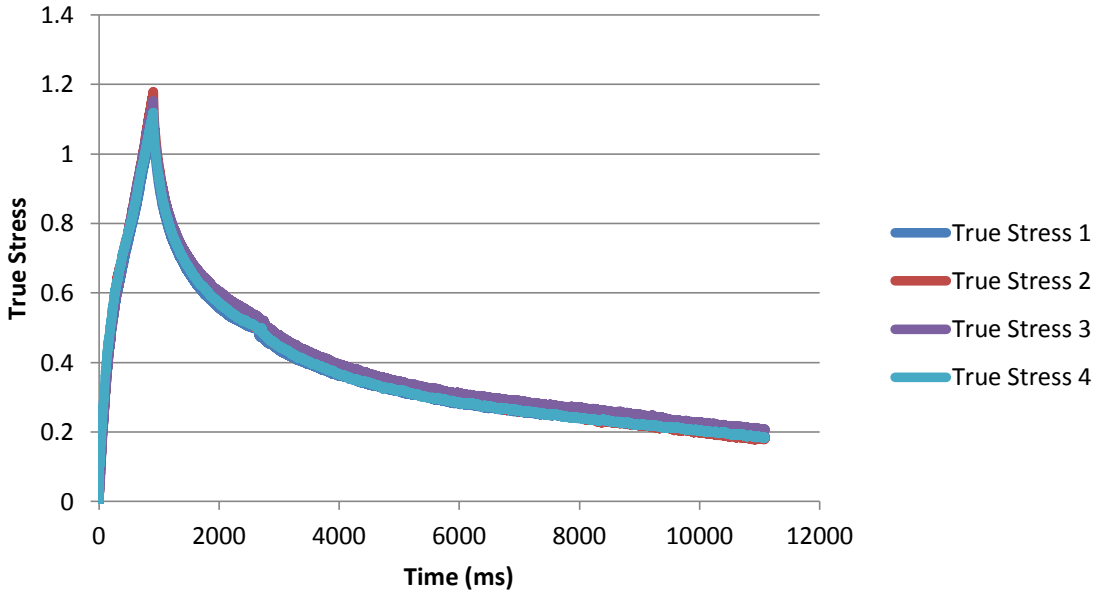

Figure 9: Four Samples tested at 135°C, 1/min and a total strain of 1.5

Experimental Findings

Over the course of the research project, a large amount of data was collected and analyzed to determine PPMA's behavior under different loading conditions and temperatures. The following sections describe some of the plots obtained from the collected data as well some that were determined after analyzing the data.

Stress vs Time

The main data that was obtained from the tests described under the testing procedure section was stress vs time. The force-displacement data collected by the Bluehill Software was used to obtain True stress under the assumption that volume remained constant in the samples. A cylinder's volume is given by

$$V = \pi r^2 h$$

where r=radius of the cylinder

h=height of the cylinder

Since volume remains constant, the radius at any time t can be calculated by equating the initial and final volumes, or in other words

$$r(t) = r_0 + \Delta r(t) = \sqrt{\frac{V}{\pi(h_0 - \Delta h(t))}}$$

where r_0= initial radius

h_0= initial height

$\Delta r(t)$= change in radius at any time

$\Delta h(t)$= total displacement at any time

Stress in a sample is equal to force over cross sectional area. The cross sectional area can be determined using the above equation and with this, the stress in the sample can be calculated as

$$\sigma(t) = \frac{F(t)}{\pi(r(t))^2}$$

where F(t) is the force at any point of time.

Utilizing this data, stress vs time curves were plotted. Figure 10 shows a plot of stress vs time at 105°C.

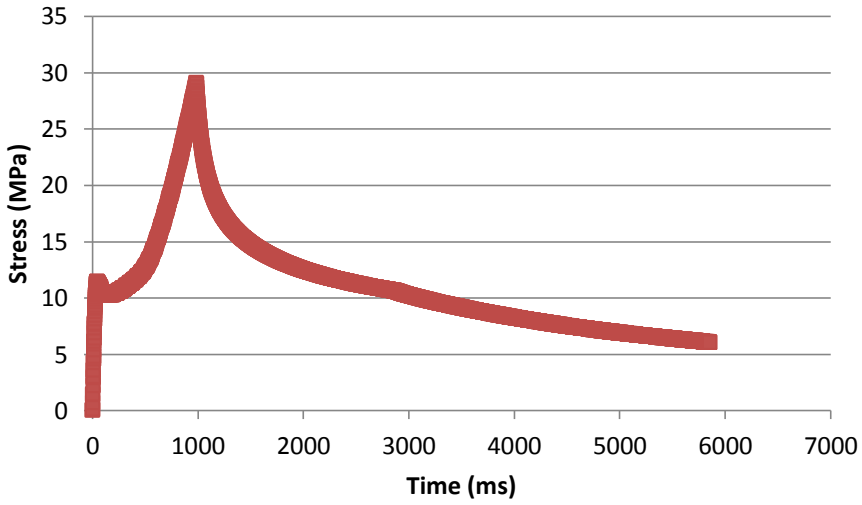

Figure 10: Stress relaxation at 105°C, 1/min and a total strain of 1.5

During the loading phase, i.e. the initial part of the curve, stress increases non-linearly with time. The yield point for samples tested at lower temperatures is easily

distinguishable in the plot along with their strain hardening behavior while the same cannot be said for samples tested at higher temperatures. This is expected as PMMA tends to be more viscous as temperature increases. When the desired strain level is attained at the end of the loading phase, the stress reaches a peak point. After this point, there is a drop in the stress values for the remainder of the test while strain is kept constant. The relation between strain input and stress output over time can be seen in the following figure.

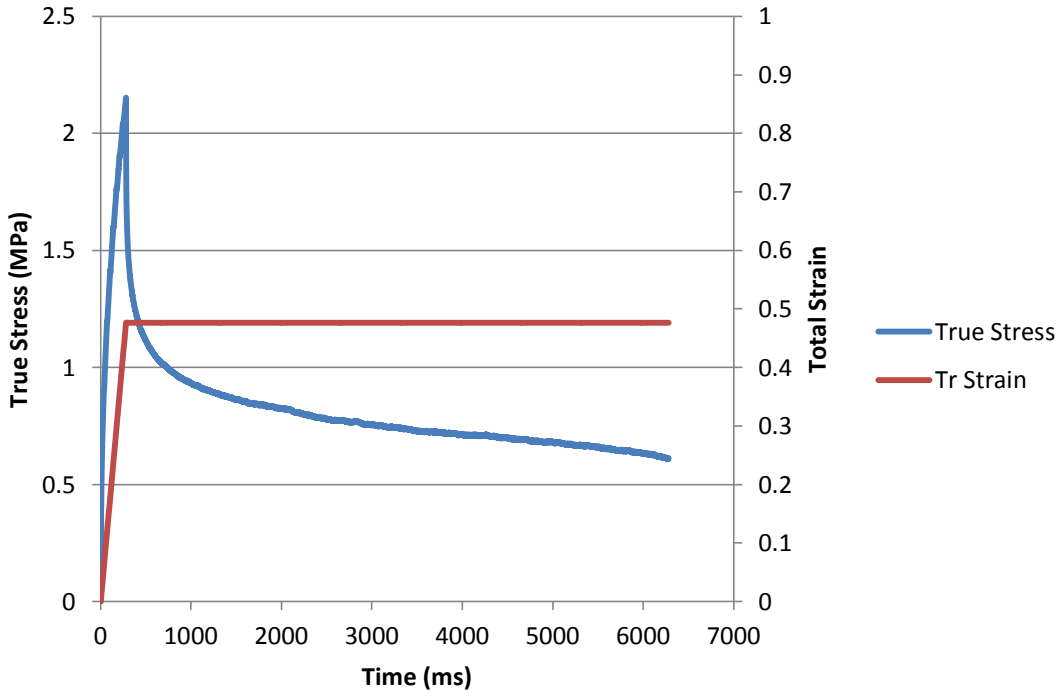

Figure 11: Stress output to strain input, 115°C, 1/min and a total strain of 0.5

As mentioned above and as can be seen in figure 11, during the loading period on the strain input profile, stress increases while the holding period relates to stress relaxation in the sample.

These stress time plots vary significantly when the test parameters are changed. The following figure shows the variation in the plots when temperature is varied between 105°C and 135°C.

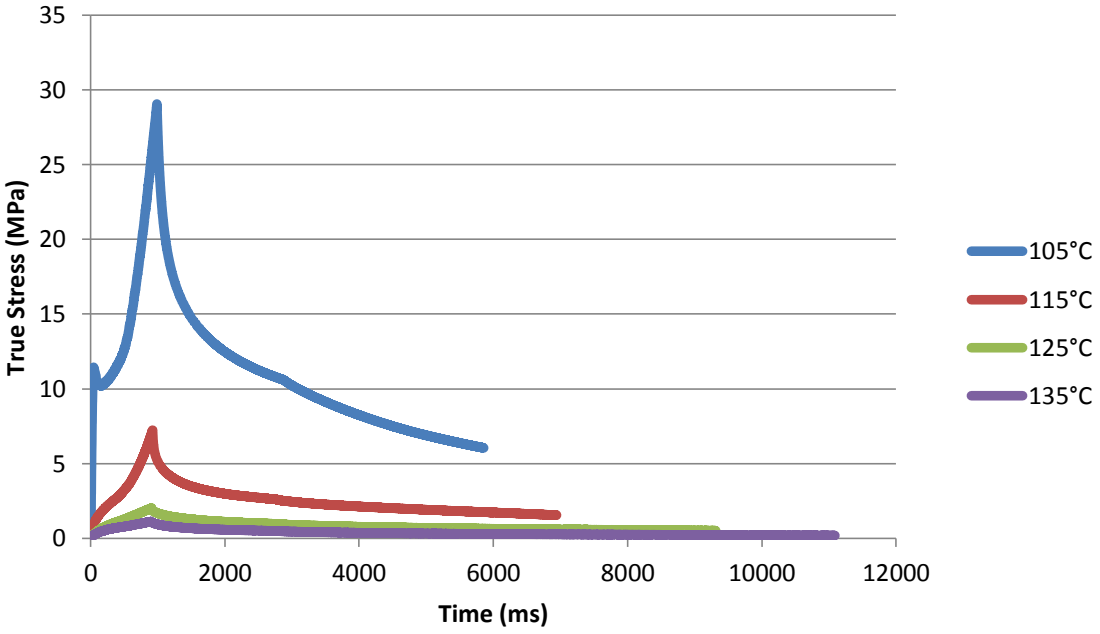

Figure 12: Stress Time plots at different temperatures, 1.0/min and a total strain of 1.5

As can be seen in the figure above, peak stress in the system decreases as temperature increases. This behavior can be attributed to compliance of PMMA at higher temperatures, a typical characteristic of polymers, and can be seen for other combinations of total strain and strain rate, figures for which can be found in the appendix.

Similarly, figure 13 depicts the behavior of PMMA when the total strain levels are varied.

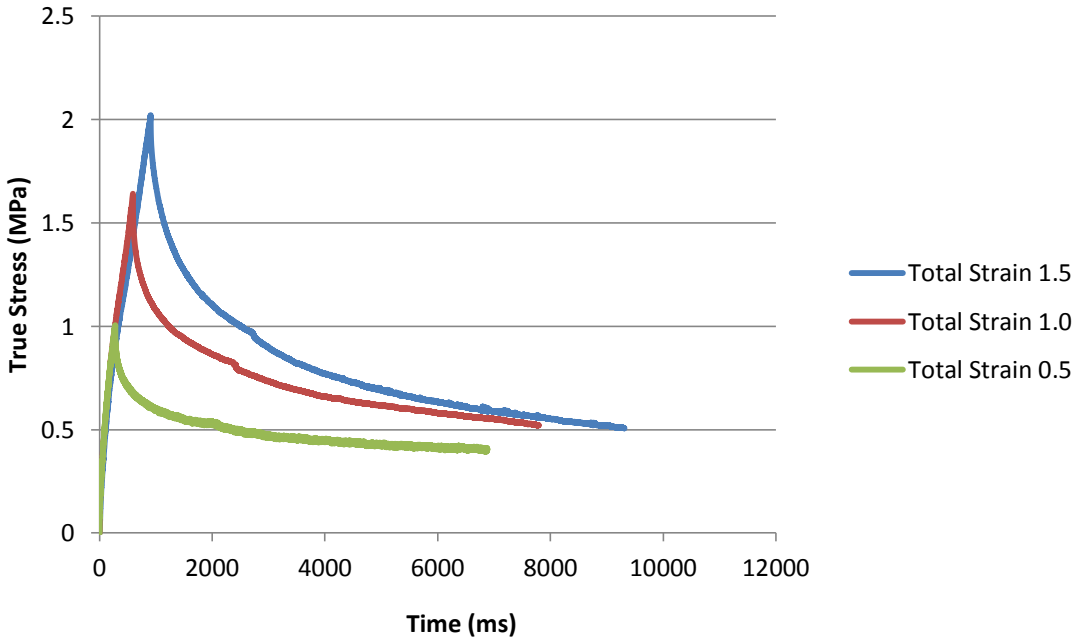

Figure 13: Stress Time plots at different total strains, 1.0/min and a temp. of 105°C

The curves in the above figure relate to samples that were tested at the same temperature and strain rate. The total strain is escalated by increasing the time under loading phase, therefore the curves follow roughly the same path till the beginning of the holding period. Hence, as total strain is increased, peak stress occurs later and higher. This trend is congruent with other combinations of temperature and strain rate, as can be inferred from the figures available in the appendix.

Figure 14 highlights the difference in behavior when strain rate is varied keeping temperature and total strain constant.

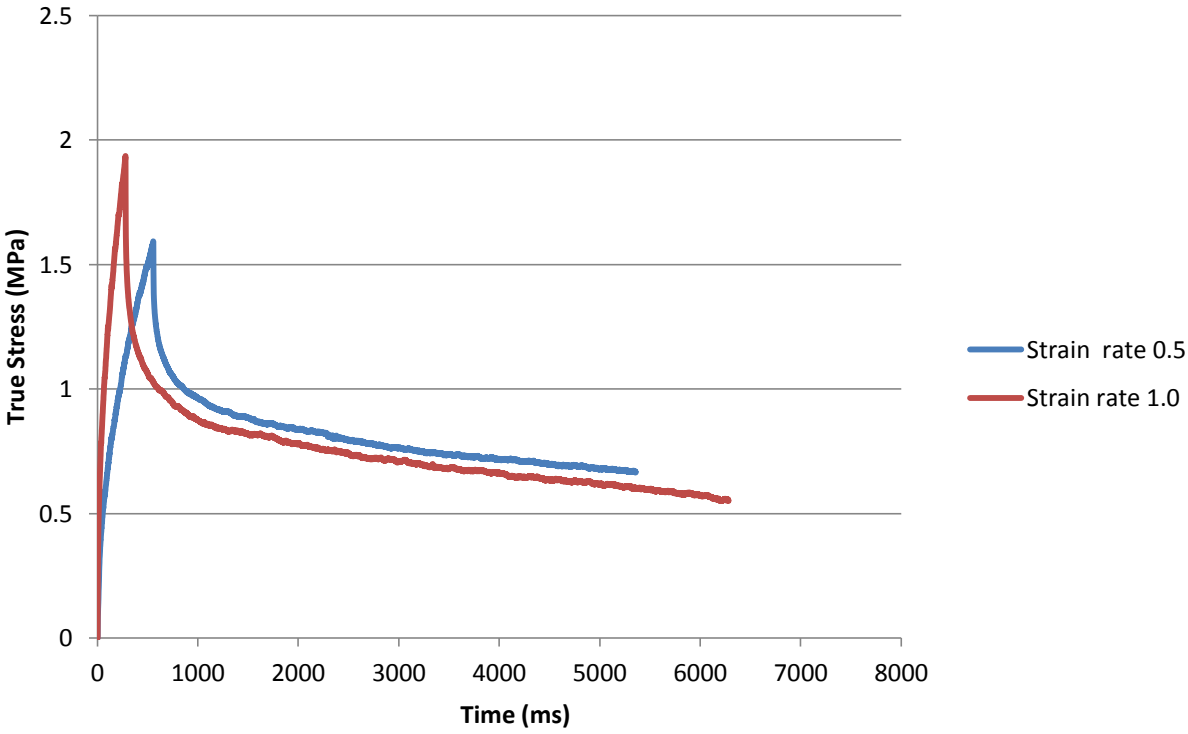

Figure 14: Stress Time plots at different strain rates, temperature of 115°C and a total strain of 1.0

The test performed at 1.0/min reaches the desired total strain value quickly compared to 0.5/min. Owing to this, peak stress associated with the strain rate of 1.0/min occurs earlier than for 0.5/min, along with a higher value. The reason for this lies in the fact that since the loading period for 0.5/min is higher, more amount of stress relaxation occurs by the time peak stress is reached.

Stress vs Strain

Since all the experiments were conducted at a constant loading rate, the shape of the stress-strain curves looks similar to the initial part of the stress time curves, i.e. the

loading period. Figure 15 shows a stress-strain curve at a temperature of 105°C, a total strain of 1.5 and a strain rate of 1.0/min.

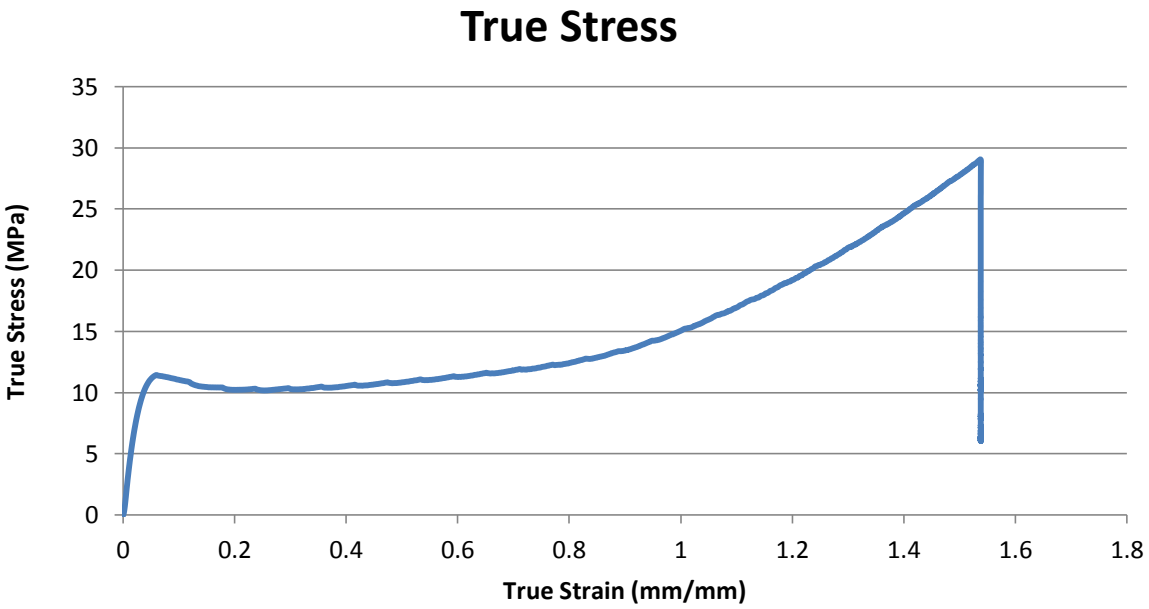

Figure 15: True Stress vs True Strain, temperature of 105°C, total strain of 1.5 and a strain rate of 1.0/min

The vertical line at the end of the curve represents stress relaxation at a constant strain. The values from this curve correspond to the stress-time values from Figure 10, and it can be seen that the loading portion of the curve is identical, with only x-values being different by a factor of the strain rate.

$$\text{Since } t = \frac{\varepsilon}{(\frac{d\varepsilon}{dt})}$$

the peak stress here occurs at a time of

$$t = \frac{1.5}{1\varepsilon/min} * \frac{60s}{min} = 60s$$

These similarities between the curves, with a vertical line at the end, is a feature accompanying all the experimental data.

Comparisons with No Cooling

Initially, before the start of this project, experiments were conducted at constant temperature to remove temperature change as a complicating factor. Comparison of one of these experiments carried out at 105 with the mechanical model can be seen in figure 16 below.

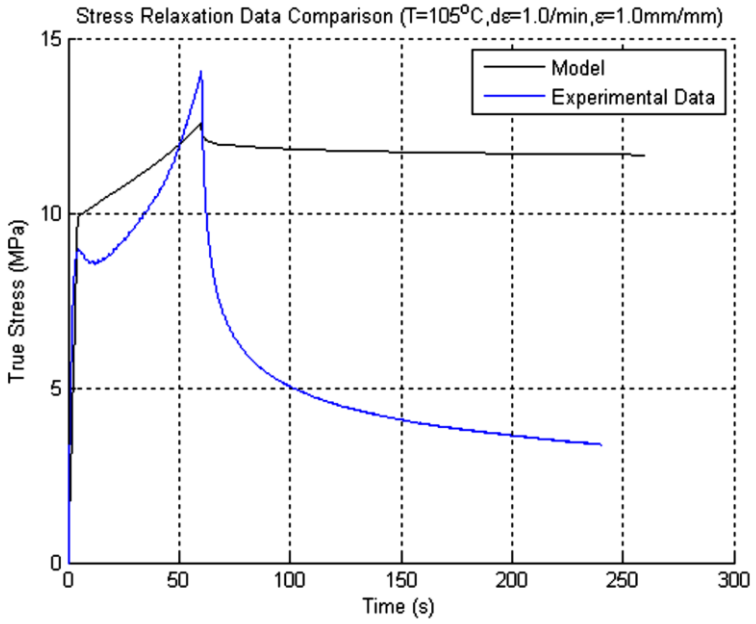

Figure 16: Stress-time data with no-cooling compared with Dupaix-Boyce mechanical model

The model predicts the behavior of the sample pretty well up to the point where relaxation begins, with the yield point and the maximum stress values on both the curves being quite close to each other. But the model fails to predict enough relaxation when compared to the experimental data. Also, cooling the sample after sufficiently loading it

more closely resembles the industrial standards of hot embossing. Therefore it was decided that cooling would be a part of the experiments to see whether an improved model could predict the difference between no cooling and cooling.

Along with performing experiments where samples were cooled by letting in air, some experiments were also conducted where samples were left at the testing temperature till the end of the experiment. These experiments were not performed as extensively as the ones with cooling, as data pertaining to similar experiments was already available. The following plot compares stress relaxation in two samples, one with cooling and the other without.

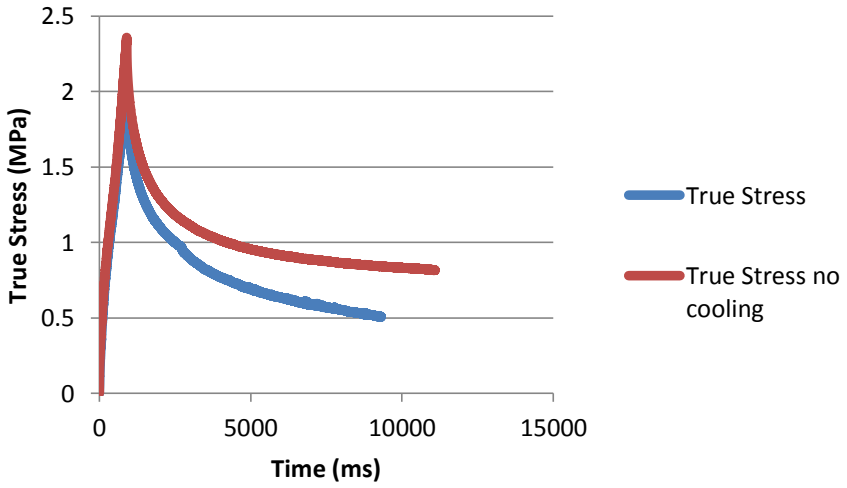

Figure 17: Stress-time data comparison between cooling and no-cooling

The experiment was performed at a temperature of 125°C, a total strain of 1.5 with a strain rate of 1.0/min. As expected, stress relaxation is more in the case of cooling

the sample. This can be attributed to thermal strain that is introduced as a result of the temperature drop when cool air is let inside the chamber.

At T=125°C, the total strain is entirely mechanical,

$$\varepsilon_t = \varepsilon_m$$

where $\varepsilon_t = Total\ strain$

and $\varepsilon_m = Mechanical\ strain$

When temperature changes, thermal strain is introduced, since it is a function of change in temperature,

$$\varepsilon_{thermal} = \alpha_{pmma}\Delta T$$

where $\alpha_{pmma} = Coefficient\ of\ thermal\ expansion$

$\Delta T = Temperature\ drop$

Therefore, total strain becomes the vector sum of mechanical and thermal strain,

$$\varepsilon_t = \varepsilon_m \pm (\varepsilon_{thermal})$$

where $\varepsilon_{thermal} = Thermal\ strain$

Now $\sigma_m \approx E\varepsilon_{el}$

where $\sigma_m = Mechanical\ stress$

$E = Modulus\ of\ elasticity$

and $\varepsilon_{el} = Elastic\ strain$

When temperature drops, thermal strain is introduced and the total mechanical strain decreases,

$$\varepsilon_{m1} = \varepsilon_{el} - \varepsilon_{thermal}$$

As a result of this, stress is now a function of the decreased strain

$$\sigma_{cooling} \approx E\varepsilon_{m1}$$

where $\sigma_{cooling} = Stress\ after\ temperature\ drop$

Finally, combining the above equations, we get

$$\Delta\sigma = \sigma_m - \sigma_{cooling}$$

This $\Delta\sigma$ is the reason for the difference in stress relaxation between the two curves in figure 14.

Extent of the Experiments

The process of hot embossing is usually done at temperatures above the glass transition temperature. Experiments were carried out at temperatures ranging from 105°C to 135°C but it was necessary to determine the temperature limits for reference as well as for future work. Figure 18 below shows stress vs time curves for samples tested at a total strain of 1.5, a strain rate of 1.0/min and at temperatures starting from 135°C up to 160°C in increments of 5°C.

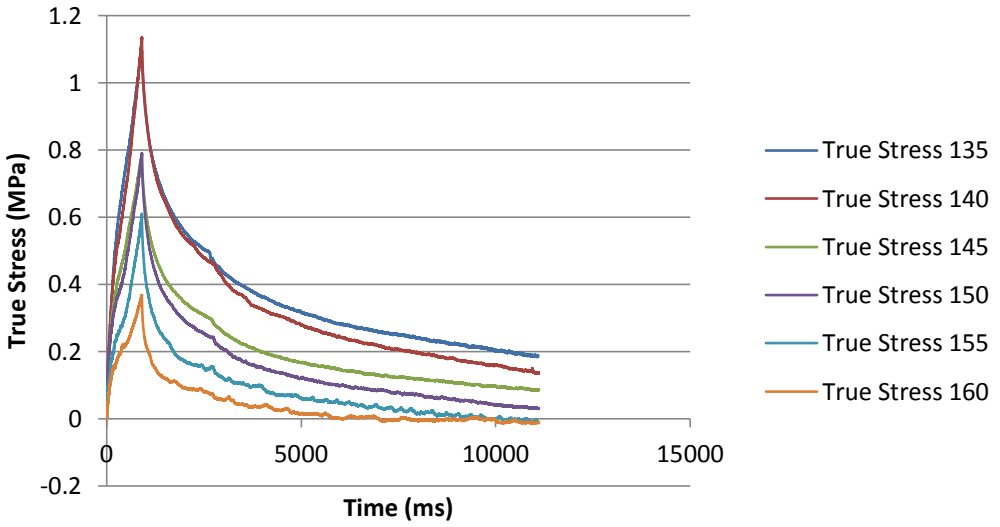

Figure 18: Stress Time plots at different temperatures, 1/min and a total strain of 1.5

The curves in figure 15 are similar in shape, as is expected, with a decrease in stress relaxation as temperature increases. At around 160°C, the stress relaxation curve relatively crosses the zero barrier into the negative stress realm when compared to curves at lower temperatures. Based on this finding, the temperature limit for hot embossing using a cylindrical PMMA sample of dimensions 8.8mm by 10mm can be said to be 160°C.

Springback

Springback is defined as the tendency of a material to attain its original shape after deformation. It is an important factor in the process of molding and, as mentioned before, had not been studied during experiments conducted in the previous project. However, there has been some research into the temperature dependent strain recovery of PMMA at small strains with no stress relaxation (Mathiesen et al, 2014). It was

discovered that there is always some amount of initial elastic recovery, while the amount of inelastic recovery is time and temperature dependent. Since large strains, stress-relaxation or cooling had not been explored, it became all the more imperative to study these aspects and their interdependence with springback.

For the experiments in this project, spring back was calculated using the following equation,

$$\%SB = \frac{h_f - h_{held}}{h_0 - h_{held}} * 100\%$$

where h_f = final height

h_{held} = height at which the sample was held

h_0 = initial height of the sample

Figure 19 below shows a pictorial representation of these heights.

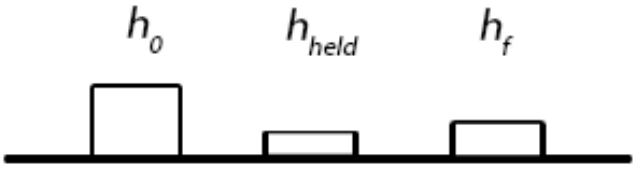

Figure 19: Height of sample during various stages of the experimental procedure

In order to avoid curling of the sample after removal of the load, they were held for different periods of time under the load. This changed the cooling time for samples tested under different combination of parameters. It was detected that cooling time was proportional to held strain and embossing temperature. Figure 20 shows a difference in spring back temperature for all embossing temperatures and held strains. It can clearly be seen from this that small held strains have release and spring back temperature greater

than large held strains owing to different cooling times. The trend reverses when it comes to temperature where high embossing temperatures have greater spring back and release temperature, even though the cooling time was more. These differences in temperature may be contributing to the spring back behavior and need to be investigated further (Mathiesen et al, 2014).

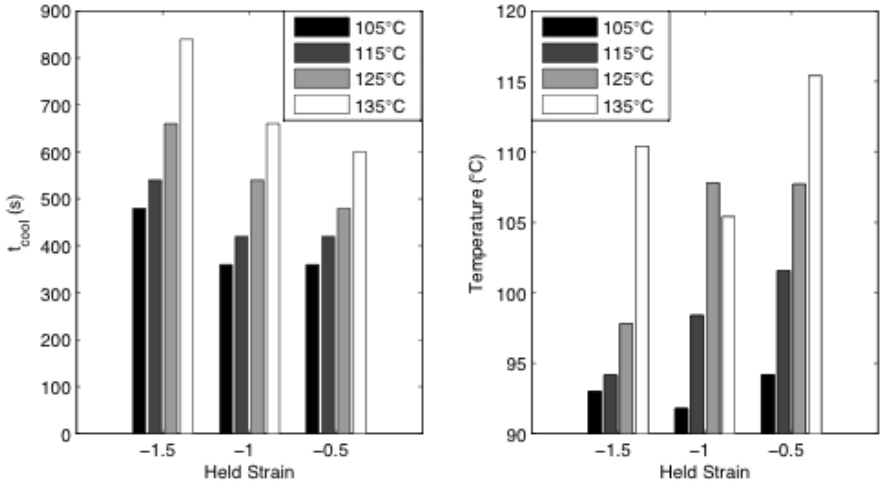

Figure 20: Cooling times and final temperatures of samples strained at a rate of -1.0/min (Mathiesen et al, 2014)

Springback was also found to be positively correlated with embossing temperature for a given held strain. On the other hand, for a given embossing temperature, it is negatively correlated with held strain. These can be inferred from the figure 21.

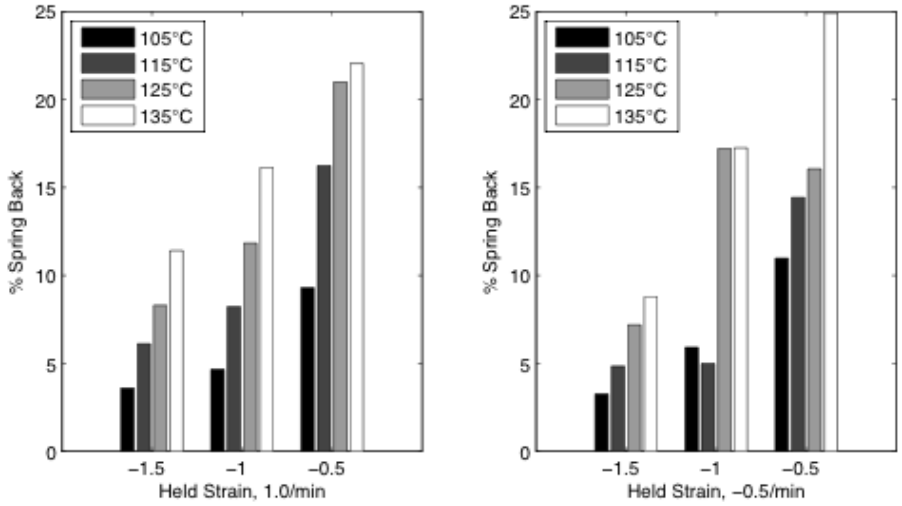

Figure 21: Spring-back of samples strained at a rate of -1.0/min and -0.5/min (Mathiesen et al, 2014)

Comparing figures 22 and 23, it can be ascertained that held strain is a more important factor than temperature for springback. This is because for small held strains, the recovery was more than three times the recovery for large held strains whereas changes in embossing temperature barely caused a 50% variation in recovery.

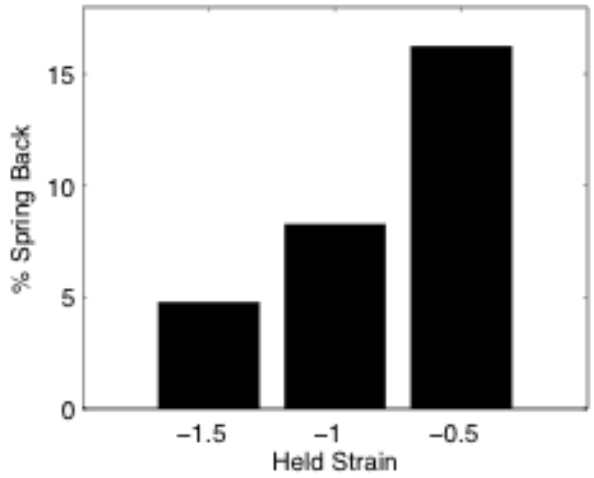

Figure 22: Springback at 115˚C with constant cooling time (Mathiesen et al, 2014)

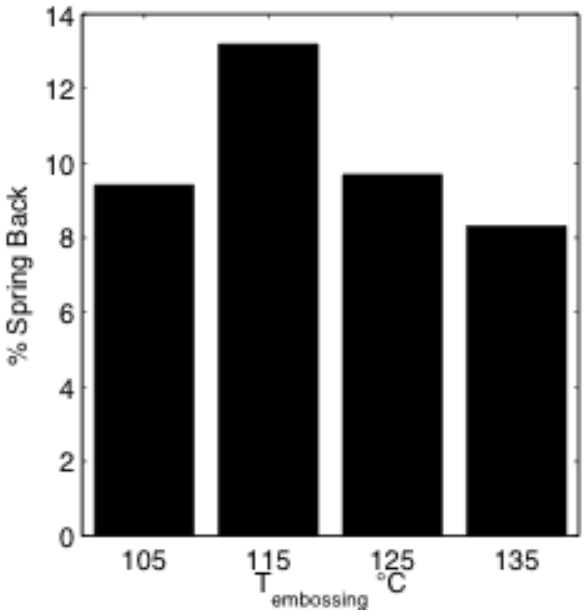

Figure 23: Spring-back at held strain of -1.0 with spring-back temp. of 100˚C

(Mathiesen et al, 2014)

Figure 23 also indicates that the relationship between temperature and springback is a fairly complex one that requires a deeper insight into the dependence on release temperature.

CHAPTER 3

Modeling

It is essential to categorize different parts of the curve according to their elasticity as this would help determine PMMA's behavior under different loading conditions and fundamentally help in modeling it. The stress-strain curves obtained after performing the experiments were fit with curves derived from hyperelastic and inelastic models. The Mooney-Rivlin model, often used to model the elastic response of rubber-like materials, was used for hyper elasticity. It is generally applied for rubbers, elastomers, and soft biological tissues. On the other hand, for inelasticity, the Chaboche model was used, which is usually adopted for plasticity in metals.

Chaboche

The Chaboche model belongs to a group of isometric constitutive models which can describe the elasto-viscoplastic behavior of materials (11). The inelastic strain rate, $\dot{E}^I$, of the simple variant of the Chaboche model can be written as:

$$\dot{E}^I = \frac{3}{2}\dot{p}\,\frac{S^I - X^I}{J(S^I - X^I)'}$$

where $\dot{p}$ describes the rate of the equivalent plastic strain and has the following form:

$$\dot{p} = \left\langle \frac{J(S^I - X^I) - R - k}{K} \right\rangle^n$$

The *k*, *R* and *K*, *n* constants are the initial yield stress, isotropic hardening and two material parameters, respectively. Tensors $S^I$and X^I are the deviatoric parts of stress and back stress tensors. The angle parameter has the following form:

$$\langle x \rangle = \frac{1}{2}(x + |x|)$$

and is called the McCauley bracket.

The $J(S^I - X^I)$ invariant is calculated from the following formula:

$$J(S^I - X^I) = \sqrt{\frac{3}{2}(S^I - X^I) : (S^I - X^I)}$$

The isotropic hardening, *R*, and kinematic hardening rate, $\dot{X}$, are defined by:

$$R = b(\dot{R}_1 - R)\dot{p}$$

$$\dot{X} = \frac{2}{3}a\dot{E}^I - cX\dot{p}$$

Where *a*,*c*,*b* and R_1 are material parameters(10).

Mooney-Rivlin

In continuum mechanics, a Mooney-Rivlin is a hyperelastic model where the strain energy density function $\boldsymbol{W}$ is a linear combination of two invariants of the left Cauchy-Green deformation tensor $\boldsymbol{B}$. The nominal or engineering strain is defined as the change in length divided by the original length:

$$\varepsilon = \frac{l_1 - l_0}{l_0} = \frac{\Delta l}{l_0}$$

Another fundamental quantity to describe material deformation is stretch ratio, denoted by λ and defined as

$$\lambda = \frac{l_1}{l_0} = \frac{l_1 - l_0 + l_0}{l_0} = \varepsilon + 1$$

Analog to the three principal strains, we obtain the three principal stretch ratios $\lambda_1, \lambda_2, \lambda_3$ from the principal axis transformation. These principal stretch ratios give rise to the deformation gradient $\boldsymbol{F}$.

$$F = \begin{bmatrix} \lambda_1 & 0 & 0 \\ 0 & \lambda_2 & 0 \\ 0 & 0 & \lambda_3 \end{bmatrix}$$

Multiplying this deformation gradient with its transverse gives us the left Cauchy-Green strain sensor, $\boldsymbol{B}$.

$$B = \begin{bmatrix} {\lambda_1}^2 & 0 & 0 \\ 0 & {\lambda_2}^2 & 0 \\ 0 & 0 & {\lambda_3}^2 \end{bmatrix}$$

Stretch invariant, $\boldsymbol{I}$, is in turn obtained from $\boldsymbol{B}$:

$$I_1 = B_{11} + B_{22} + B_{33} = {\lambda_1}^2 + {\lambda_2}^2 + {\lambda_3}^2$$

Similarly $$I_2 = {\lambda_1}^2{\lambda_2}^2 + {\lambda_2}^2{\lambda_3}^2 + {\lambda_1}^2{\lambda_3}^2$$

$$I_1 = {\lambda_1}^2{\lambda_2}^2{\lambda_3}^2$$

The stretch invariants, I_1& I_2, together constitute the Mooney-Rivlin equation:

$$W = C_1(I_1 - 3) + C_2(I_2 - 3)$$

The Cauchy stress tensor ***T***, is given by:

$$T = -pI + 2\frac{\partial W}{\partial I_1}B - 2\frac{\partial W}{\partial I_2}B^{-1} \quad (1)$$

Also, with the absence of shear, $$T=\begin{bmatrix} \sigma_x & 0 & 0 \\ 0 & \sigma_y & 0 \\ 0 & 0 & \sigma_z \end{bmatrix} \quad (2)$$

Differentiating the energy density function and substituting in (1), we get:

$$T = -pI + 2C_1B - 2C_2B^{-1} \quad (3)$$

Equating (2) and (3)

$$\begin{bmatrix}\sigma_x & 0 & 0\\ 0 & \sigma_y & 0\\ 0 & 0 & \sigma_z\end{bmatrix}=\begin{bmatrix}-p & 0 & 0\\ 0 & -p & 0\\ 0 & 0 & -p\end{bmatrix}+2C_1\begin{bmatrix}{\lambda_1}^2 & 0 & 0\\ 0 & {\lambda_2}^2 & 0\\ 0 & 0 & {\lambda_3}^2\end{bmatrix}-2C_2\begin{bmatrix}{1}/{{\lambda_1}^2} & 0 & 0\\ 0 & {1}/{{\lambda_2}^2} & 0\\ 0 & 0 & {1}/{{\lambda_2}^3}\end{bmatrix}$$

$$\sigma_x = -p + 2C_1{\lambda_1}^2 - 2\frac{C_2}{{\lambda_1}^2}$$

$$\sigma_y = -p + 2C_1{\lambda_2}^2 - 2\frac{C_2}{{\lambda_2}^2}$$

$$\sigma_z = -p + 2C_1{\lambda_3}^2 - 2\frac{C_2}{{\lambda_3}^2}$$

Ansys was used for fitting stress-strain curves obtained from the experiments. The following three figures show the Chaboche curve fit to a stress-strain curve for a sample tested at 135°C, true strain of 1.5 and a strain rate of 1.0/min:

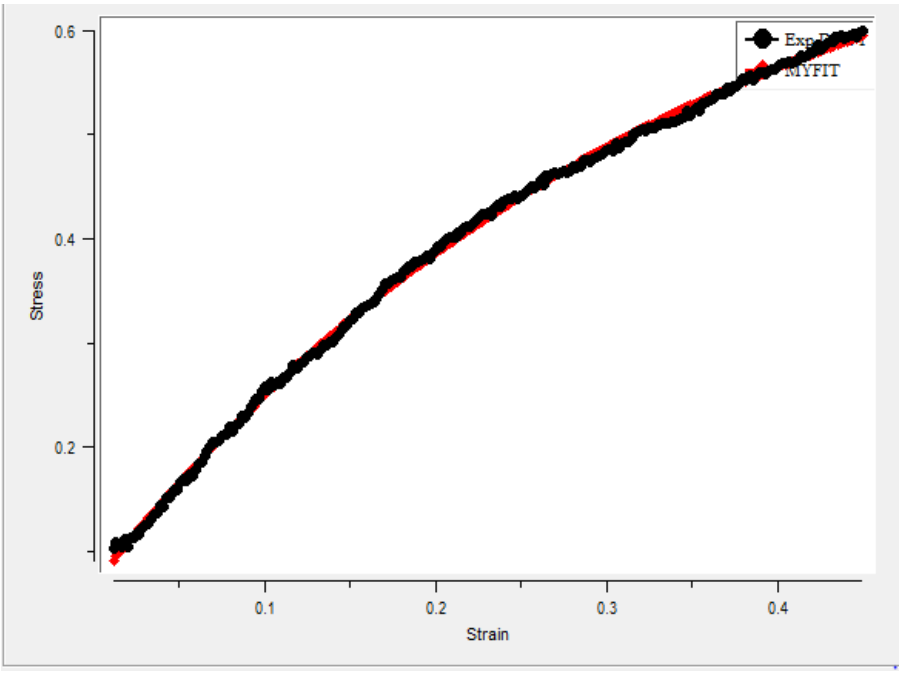

Figure 24: Chaboche curve fit till a strain of 0.5 for a stress-strain curve at 135°C, ts=1.5 and strain rate=1.0

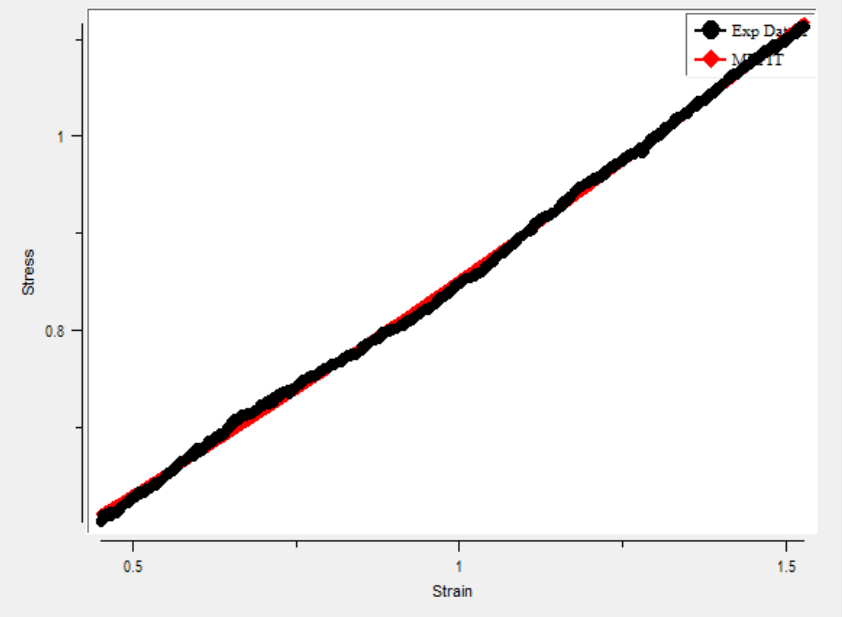

Figure 25: Chaboche curve fit from a strain of 0.5 to 1.5 for a stress-strain curve at 135°C, ts=1.5 and strain rate=1.0

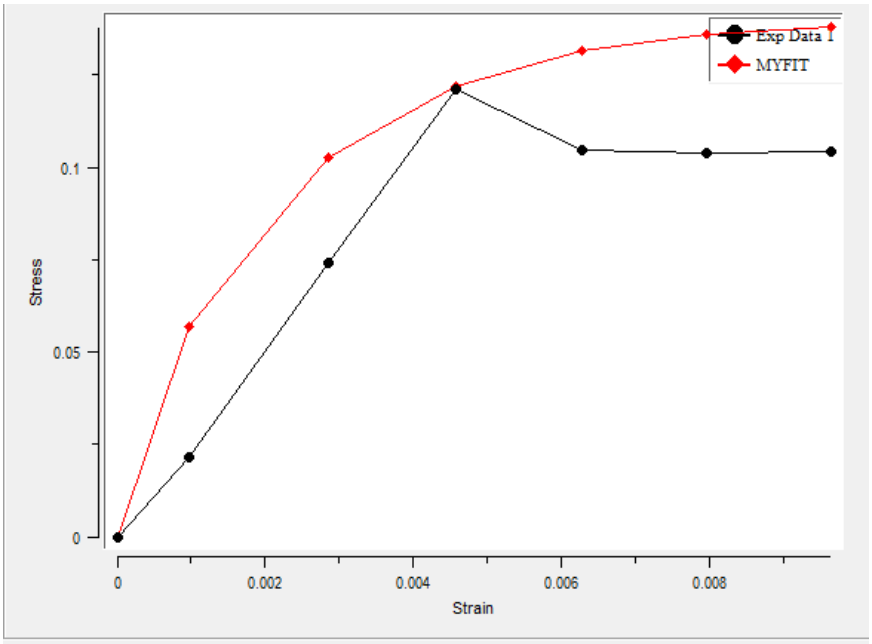

Figure 26: Chaboche curve fit till a strain of 0.01 for a stress-strain curve at 135°C, ts=1.5 and strain rate=1.0

The stress-strain curve was divided into three different parts on the basis of strain:

1) 0 to 0.01
2) 0.01 to 0.5
3) 0.5 to 1.5

This was done to determine the elasticity of different parts of the curve. From figure 26, it can be said that the Chaboche inelastic curve does not fit the initial part of the experimental curve well. This called for a curve fit using the Mooney-Rivlin model, which can be seen in figure 27 below.

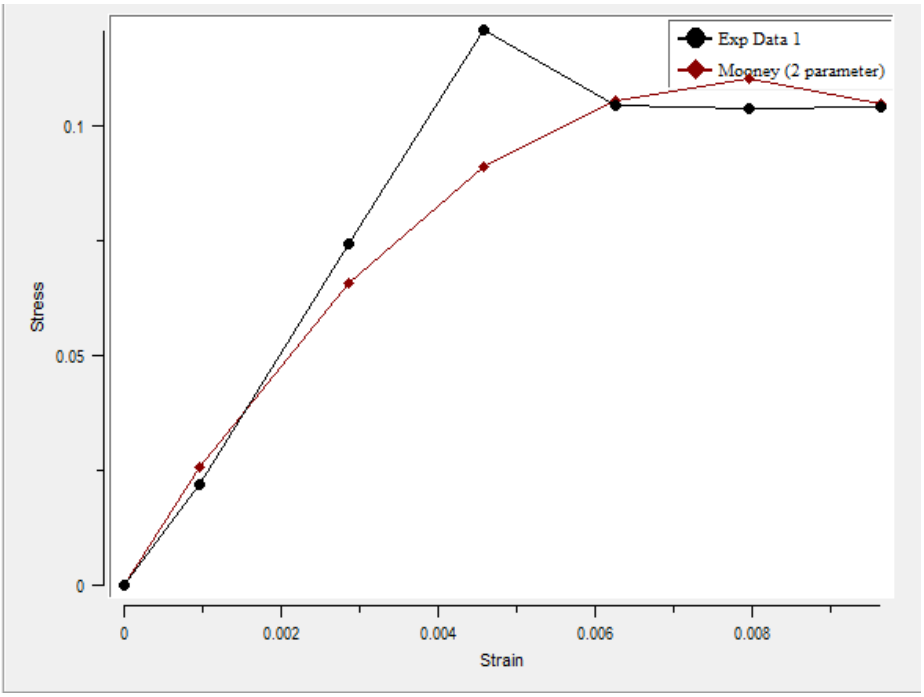

Figure 27: Mooney-Rivlin curve fit till a strain of 0.01 for a stress-strain curve at 135°C, ts=1.5 and strain rate=1.0

The Mooney-Rivlin curve fits the experimental curve much better compared to the Chaboche model.

Similar calculations were performed for a sample tested at 115°C, true strain of 1.5 and a strain rate of 1.0/min. The following figures show the curve fits:

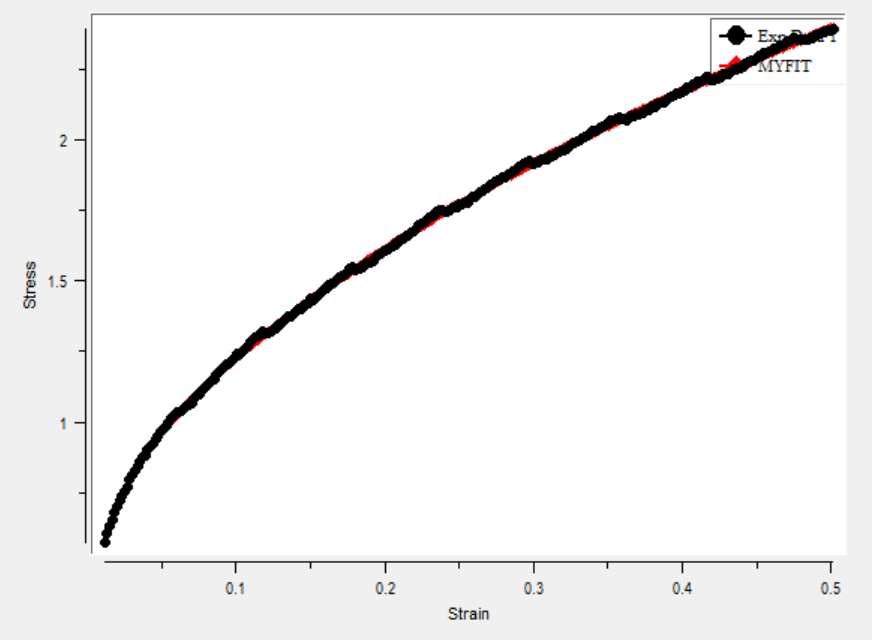

Figure 28: Chaboche curve fit till a strain of 0.5 for a stress-strain curve at 115°C, ts=1.5 and strain rate=1.0

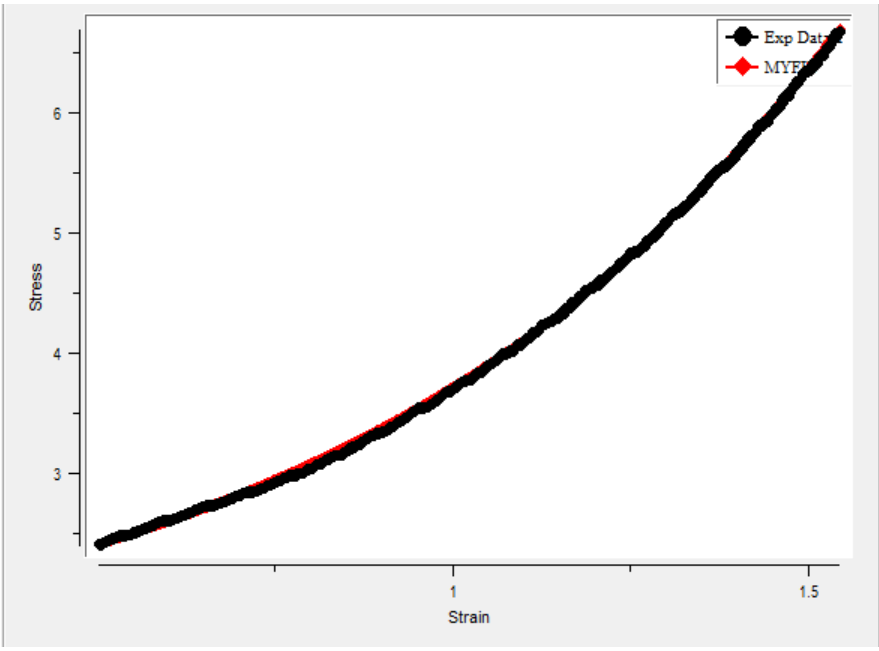

Figure 29: Chaboche curve fit from a strain of 0.5 to 1.5 for a stress-strain curve at 115°C, ts=1.5 and strain rate=1.0

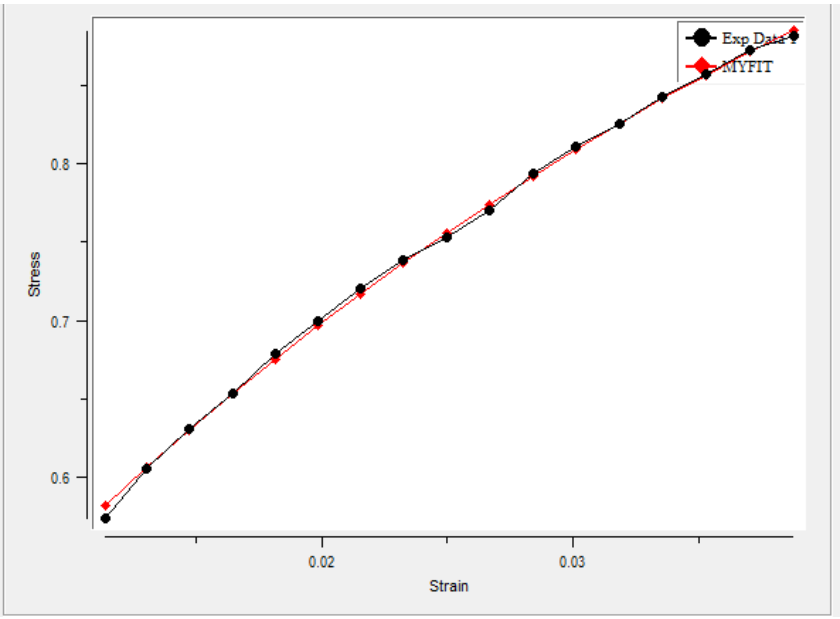

Figure 30: Chaboche curve fit till a strain of 0.01 for a stress-strain curve at 115°C, ts=1.5 and strain rate=1.0

These figures indicate that the Chaboche curve almost overlaps the data obtained at 115°C, total strain of 1.5 and a strain rate of 1.0 /min. Similar comparisons were made for data obtained at 105°C and 125°C, total strain of 1.5 and a strain rate of 1.0/min. These comparisons reiterate the fact that an inelastic model curve fits the experimental data pretty well upto a certain temperature range, beyond which a hyperelastic model curve has to be introduced to get the complete picture.

Although these models can be used for curve fitting the loading curve, they are not suitable for detecting springback because of the following reasons:

1) Chaboche model is perfectly plastic

For this reason, there will be no time dependence in the unloading part-the stress will instantaneously decrease when the load is removed instead of gradually decreasing with time.

2) Mooney- Rivlin model is completely elastic

   Hence, the material will completely spring back to its original shape upon loading.

Also, it was clear that the previous models would not provide an adequate amount of stress during relaxation because they were lacking an element that represented back stress, a critical factor leading to the majority of the springback upon load removal. Therefore, a new model is being developed, based off of the Dupaix-Boyce model, to capture the springback due to time dependent relaxation.

Model Comparisons

The current mechanical model, being developed by Mathiesen-Dupaix, is a three-dimensional model using three parallel resistances to imitate intermolecular and network interactions as shown in figure 31.

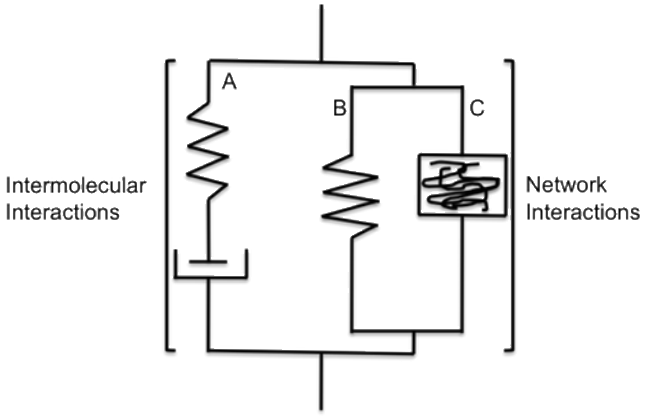

Figure 31: Mathiesen Model (Mathiesen et al, 2014)

The deformation gradient in resistance A is multiplicatively broken down into its elastic and plastic components, which are further decomposed into stretch and rotational components using polar decomposition. Resistance B consists of an 8-chain hyperelastic model that provides back-stress while resistance C consists of a Rolie-Poly element with finite extensibility (Mathiesen et al, 2014).

Modifications were made to this model to incorporate cooling and data from this was fit to the stress relaxation data obtained from the experiments. It was observed that the model predicts the uniaxial compression behavior of the material, prior to relaxation, very well. This is consistent across all test parameter combinations, namely temperatures and strains. While there's no particular trend for a total strain of 1.0, for 1.5, the model's prediction of stress relaxation changes from overestimation to underestimation as the temperature increases, with an almost perfect prediction at 115°C. This behavior can be seen in the following figures,

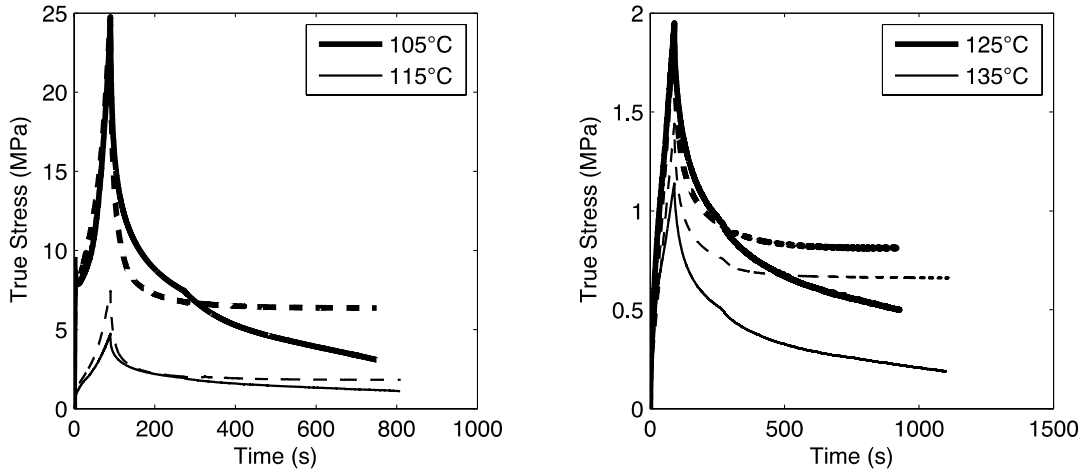

Figure 32: Comparisons of Mathiesen model with experimental data, strain rate of 1.0/min and held strain of 1.5 (Mathiesen et al, 2014)

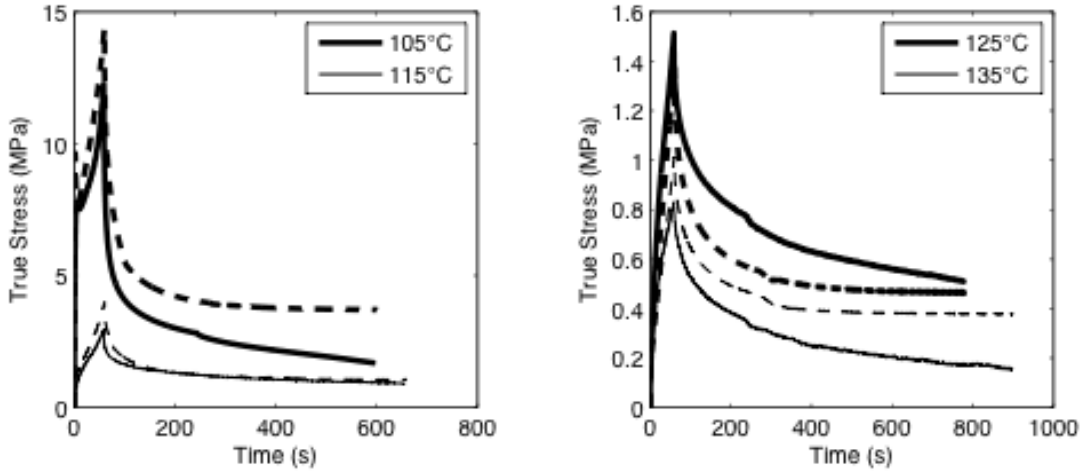

Figure 33: Comparisons of Mathiesen model with experimental data, strain rate of 1.0/min and held strain of 1.0 (Mathiesen et al, 2014)

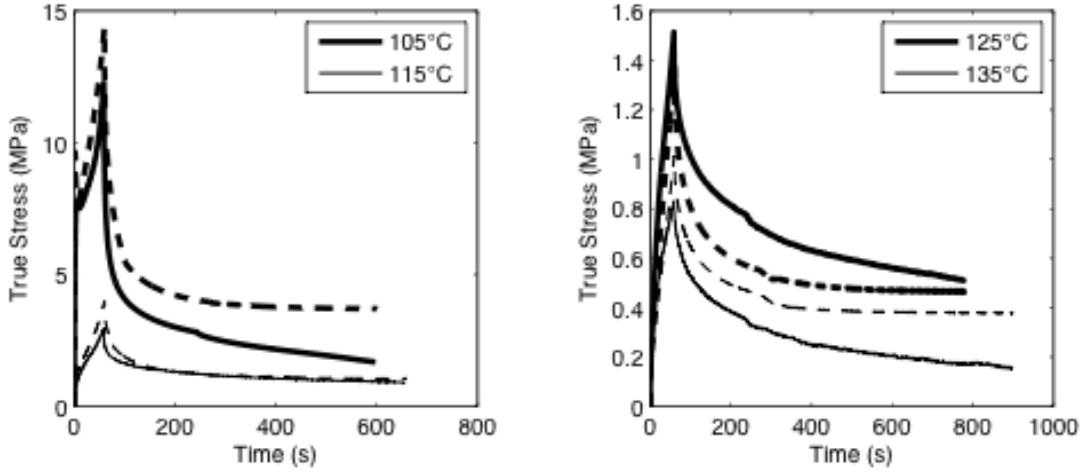

Figure 34: Comparisons of Mathiesen model with experimental data, strain rate of 1.0/min and held strain of 0.5 (Mathiesen et al, 2014)

When comparing this data with model comparisons made before the start of this project, it can be concluded that the current model is significantly better at predicting PMMA's behavior during the process of hot embossing.

CHAPTER 4

The objective of this section of the project was to determine whether the theoretical data and values obtained from the stress-strain experiments could be applied to real world situations. Experiments were performed on PMMA substrates using molds made from silicon and containing micro-channel patterns. LabView was used to write a program which used the parameters controlling the experiments as input to output the temperature at each stage of the experimental process along with the displacement of the sample. This pattern, after being embossed on the substrate, was analyzed under a microscope to determine its uniformity as well as any changes it underwent, such as spring back, with time. Figure 35 shows two of these patterns embossed on a PMMA substrate.

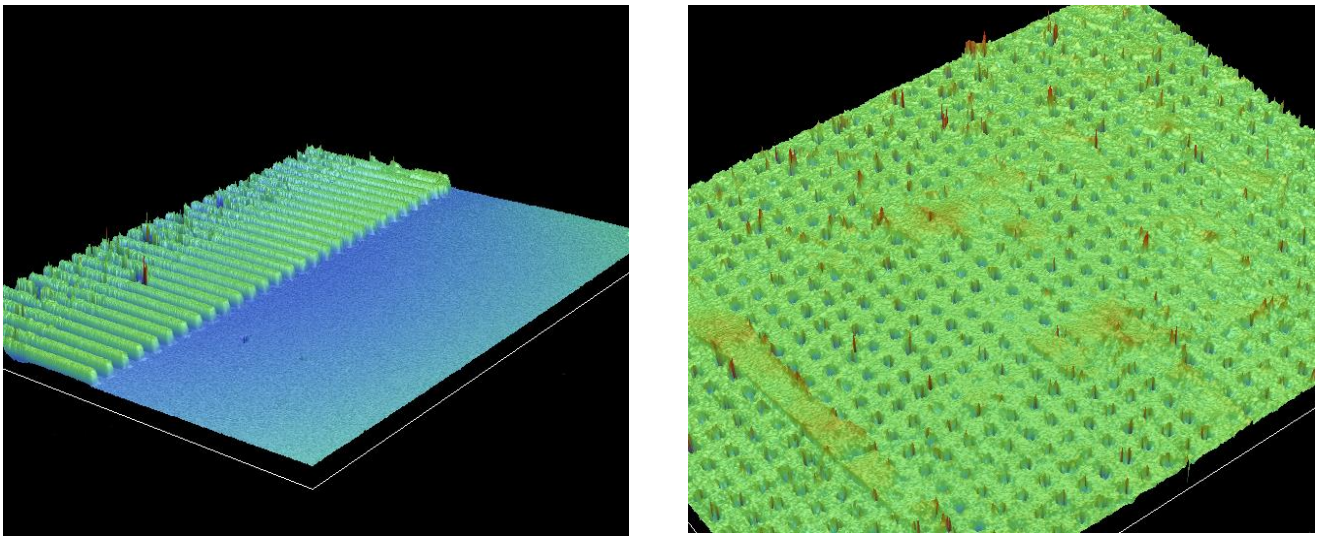

Figure 35: Mold Patterns

Equipment Used

The samples of PMMA used for these experiments were essentially the same as the ones used for the stress-strain experiments. These measured 4.4mm in height and 10mm in diameter. The main reason behind reducing the height of the samples was to make it easier to run simulations as well as get finer patterns on the substrates. Figure 36 shows an example of a specimen before and compression.

Figure 36: Undeformed and deformed PMMA samples

In order to compress these samples, a compression machine built by Greg Firestone of the Integrated and Systems Engineering Department of The Ohio State University was used. This machine consists of a heating where the sample is heated. The system also consists of a static upper plate and a movable lower plate, with both of them located inside the heating chamber. This setup is in turn connected to a computer having LabView and a controller run by a program called Green Series that helps input the initial temperature of the chamber. A program created on LabView was then used to input parameters that define these experiments. This program recorded the displacement of the

lower compression plate as well as data from a load cell that was set up to detect the amount of force being applied at a particular point of time. These force and displacement data were then used in simulations to determine whether the experimental knowledge could be transferred over to the practical side as well.

LabView Program

A LabView program was developed by Peng He of the ISE Department of OSU in order to aid the process of hot embossing using the machine developed by Greg Firestone. A sample program view is shown in figure 37.

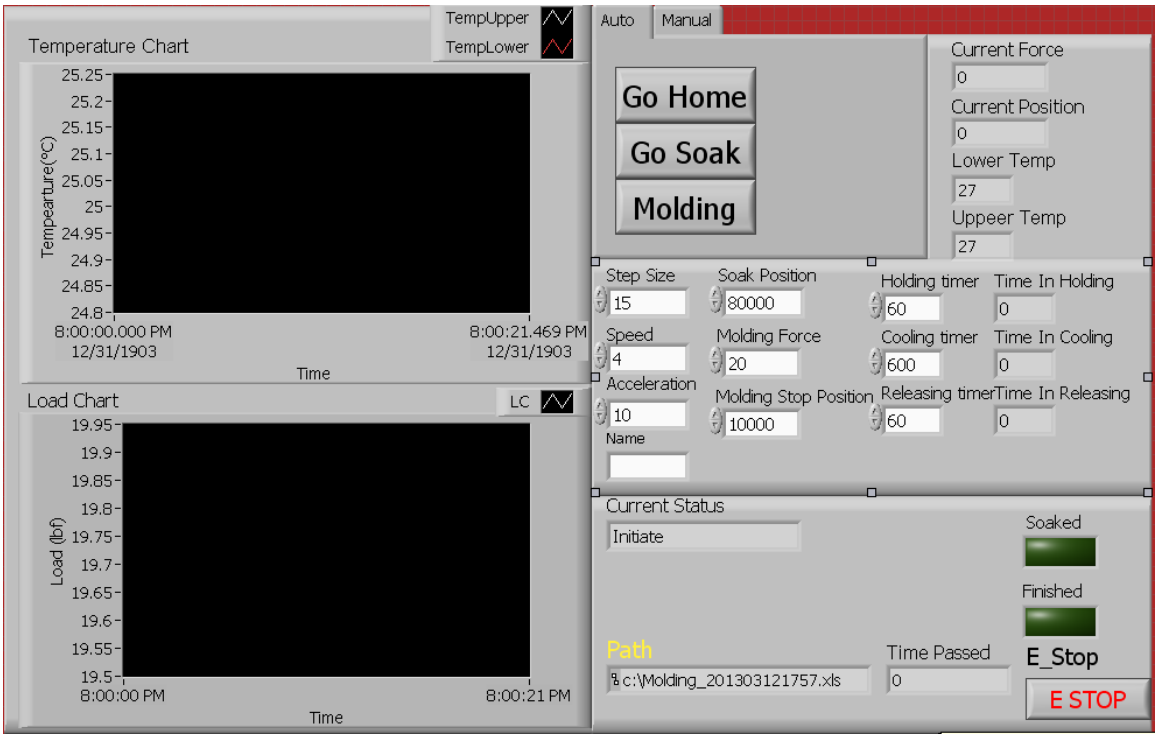

Figure 37: LabView program controlling the embossing process

The distance moved by the lower compression rod is measured in terms of steps where 1mm=1650 steps. Before the molding process starts, the plate is brought to a position which is just below the point of contact of the sample and the upper plate. This position corresponds to 86000 steps and is known as 'Soak Position'. The final position of the plate is 96000 but is ultimately based on the height of the sample being tested. Ideally the height of a sample should be 4.4mm, but human error while machining the samples results in the height being a few tenths of a millimeter more or less than 4.4mm. Accordingly the number of steps to be added or subtracted from 96000 is calculated.

$$1mm = 1650\ steps$$

$$10\mu m = 16.5\ steps$$

$$\text{Height of sample} = 4.4mm \pm x\ mm$$

$$\text{Final position of plate} = 96000 \mp (x * 1650) steps$$

Finally, molding force is entered in the program, usually in multiples of 10 *lbf*.

Testing Procedure

The method used to test the samples is as follows:

1. Input parameters in the hot embossing program created using LabView. This consists of molding force, start and final position of the lower plate and the time for cooling the sample.

2. The lower compression plate is brought to its starting position, also known as 'Home'.

3. A hot embossing mold is cleaned using a soft tissue to remove any dust particles and placed on the lower compression plate.

4. Input temperature by adding 10°C to the desired temperature.

5. Turn on the power on the controller using the green switch.

6. Send program to the controller by clicking on the 'download to controller' icon.

7. Execute the program by clicking on 'Execute'.

8. Move the compression plate to the 'Soak Position'.

9. On the controller, press the 'Reset' button. You will hear a noise confirming the program has registered.

10. Press and hold the 'PRG 1' button on the controller till the LED located below the name turns green.

11. Wait for 20 minutes for the sample to heat up to the input temperature.

12. After 20 minutes, the chamber and the sample should reach the input temperature. This is indicated by the temperature reading on the controller.

13. Click on 'Molding' in the LabView program to start the process of molding.

14. After the process is finished, a dialog appears asking the user to start the cooling process. Press the 'SET/ENT' button on the controller twice, then the 'UP' button and finally the 'SET/ENT' button again. The chamber begins to cool down to room temperature.

15. When the temperature reaches 70°C, slowly get the lower compression plate to its initial position using manual controls in the LabView program.

16. Remove the sample from the chamber. Output data is automatically saved in an excel file in a pre-defined location on the computer.

17. Place the sample under a surface profiler to study the micro-channels embossed on the polymer substrate.

18. Capture the image as well as the width of the micro-channels using a software called Vision.

Experiments

Various combinations of force and temperature were used for these hot embossing experiments. The following test matrix details these combinations:

Table 2: Test matrix (blue portion=test combination)

Force (*lbf*)	**Temperature (°C)**			
	115	125	135	145
10				
20				
30				
40				

Samples were not tested with forces of 10 lbf at 115°C and 125°C as it was not sufficient enough to emboss distinct micro-channels on the PMMA substrates.

The hot embossed samples were put under a surface profiler to get images that clearly defined the width of the micro-channels as well as show the shape of these micro-channels. Figure 38 shows an image of micro-channels embossed on one of the samples tested at 135°C using a force of 25 *lbf*.

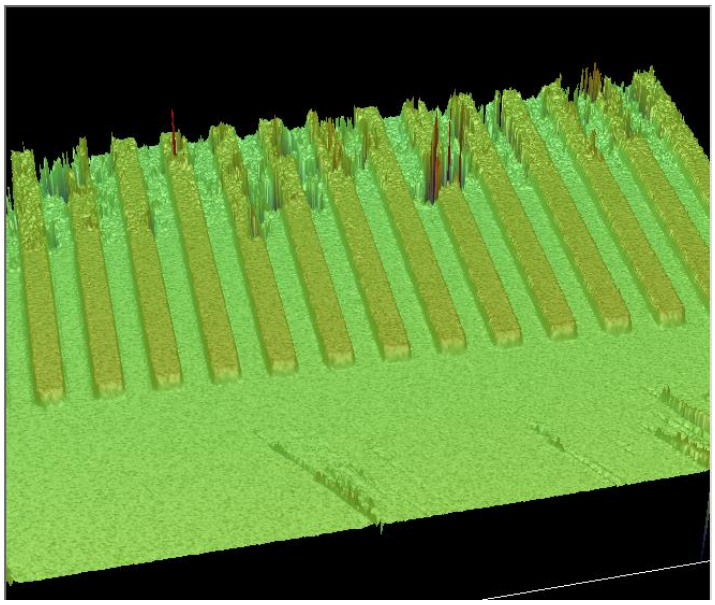

Figure 38: 3D view of micro-channel pattern

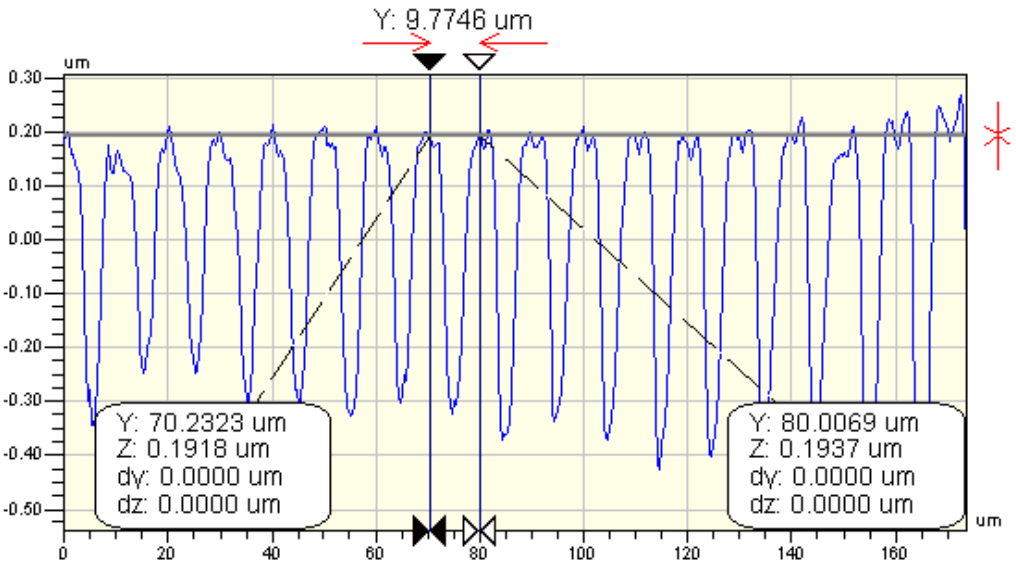

Figure 39: Data showing width of micro channel

It was also discovered that the embossing process became easier as the temperature was increased. Samples, when being tested at $T_{g,}$ would not go upto the final position of 96000 steps

no matter how much the force was increased. This behavior is expected as polymers transition from viscoelastic solids to semi viscous fluids as temperature is increased beyond their glass transition temperature.

CHAPTER 5

Conclusions

Most of the characteristics of the material's stress-time behavior were similar to what was expected from large-strain relaxation tests on polymers. In particular, the changes in behavior observed based on variation of the test parameters were not unexpected. Nonetheless, since there was a lack of quantifiable relaxation data with cooling for PMMA at large strains, and in general for the process of hot embossing, the data from these tests will be useful in enhancing the material model to better predict and represent PMMA's behavior under complex loading conditions.

These tests yielded some unexpected results as well. To begin with, the tests churned out highly repeatable results, thus cementing the fact that the relaxation data is predictable to a great degree given the right mechanical model. Additionally, temperature dependence turned out to be more linear than was expected for temperatures above T_g. Along with this, the temperature limit for the process of hot embossing was determined to be 160°C. The ability to be able to predict PMMA's behavior at temperatures well above T_g for applications involving hot-embossing could be very important and can prove to be very useful in the future.

Previous experiments, conducted by students before the start of this project, did not include some basic aspects of hot embossing in their procedure. One of these was cooling the sampling, which is quite significant in any molding process. Hence the material model did not reproduce stress relaxation as seen in the experimental results; in

particular, it failed to predict enough stress relaxation. Additionally, one important aspect of hot embossing that was not included in the mechanical model was spring back of the material after a load was removed. This could lead to incorrect prediction of springback in the polymer substrate, especially when using a material model to determine mold geometry and procedure in hot embossing. Erroneous prediction of springback can lead to situations where the mold geometries would seem to produce the desired surface profile but actually produce flawed profiles.

Factoring in these aspects made it possible to make some noteworthy changes to the mechanical model. This model, based on industrial standards of hot embossing, predicts data better than the previous models, which was the ultimate aim of this project. Further investigation of the collected data will also help better predict springback and ultimately reduce trial and error in the mold design procedure, thereby saving time and money.

Future Work

There is considerable scope for future elaboration of the work that started with this project. To begin with, a large amount of systematic editing of the material model can be done so that it continues to represent the material's behavior under different loading conditions. More springback data needs to be collected to better incorporate it into the mechanical model. Once these changes have been made, more experiments can be performed to authenticate the accuracy of the model. Load based molding experiments can be performed on an extensive scale along with displacement based experiments to get a better insight into PMMA's behavior during the process of hot embossing.

Cell development is another area where the study of the process of stress relaxation on polymers would be useful. Cells thrive within a certain threshold of environmental stress, and determining the perfect situation for a cell to thrive on a fiber mat made out of polymers is highly dependent on the polymers mechanical model. Collaborating with students from the Chemistry Department of the Ohio State University, a project was carved out that focuses on developing simple finite element models of the interaction between cells and electro-spun fiber mats. The simplest of these models involved an axisymmetric model of the fiber mat with a thin layer of matrigel on top. Taking it a step further to involve complex symmetries and other parameters involved would help in applying the results from these simulations and experiments to real world conditions.

Stress relaxation in PMMA has a wide scope with a lot of interesting stuff that is yet to be experimented upon. Hopefully, the details obtained as a result of this project

will be able to supplement the work previously done in this area and open up doors for further development in other related fields as well.

References

1) Ambroziak, Andrzej and Pawel Klosowski. 2006. "The Elasto-Viscoplastic Chaboche Model." *Task Quaterly* 10(1):49-61. Retrieved from http://www.task.gda.pl/files/quart/TQ2006/01/TQ110H-E.PDF

2) Ambroziak, Andrzej. 2005. "Numerical Modeling of Elasto-Viscoplastic Chaboche Constitutive Equations Using MSC.Marc." *Task Quaterly* 9(2):157-166. Retrieved from http://www.researchgate.net/publication/233757908_NUMERICAL_MODELING_O F_ELASTO-VISCOPLASTIC_CHABOCHE_CONSTITUTIVE_EQUATIONS_USING_MSC.MARC/file/9fcfd50b466733a949.pdf

3) Cavette, Chris. (n.d.). *Acrylic Plastic*. Retrieved from http://www.enotes.com/topics/acrylic-plastic.

4) Chen Y., Luyan Zhang and Gang Chen. (2008, April 2). Fabrication, modification, and application of poly(methyl methacrylate) microfluidic chips. *ELECTROPHORESIS* 29 (9):1801–1814. DOI: 10.1002/elps.200700552.

5) Ghatak, Arindam and Rebecca Dupaix. 2010. Material Characterization and Continuum Modeling of Poly (Methyl Methacrylate) (PMMA) above the Glass Transition [Abstract]. *INTERNATIONAL JOURNAL OF STRUCTURAL CHANGES IN SOLIDS – MECHANICS AND APPLICATIONS* 2(1):53-63.

6) Ghatak, Arindam and Rebecca Dupaix. 2010. "Material Characterization and Continuum Modeling of Poly (Methyl Methacrylate) (PMMA) above the Glass Transition ." *INTERNATIONAL JOURNAL OF STRUCTURAL CHANGES IN SOLIDS – Mechanics And Applications* 2(1):53-63. Retrieved from http://journals.tdl.org/ijscs/index.php/ijscs/article/view/2352.

7) Hot Embossing. (n.d.). *MEMS And Nanotechnology Exchange.* Retrieved October 4, 2013 from https://www.mems-exchange.org/catalog/hot_embossing/.

8) Mathiesen D, Kakumani A and Dupaix R. 20014. "Characterization and modeling of temperature and strain dependent spring-back of Poly(methyl methacrylate) (PMMA)." To be published.

9) Polymethyl methacrylate (PMMA). (n.d.). In *Encyclopedia Britannica online.* Retrieved from http://www.britannica.com/EBchecked/topic/1551203/polymethyl-methacrylate- PMMA

10) Rivlin, R.S. 1949. "Large Elastic Deformations of Isotropic Materials. V. The Problem of Flexure." *Proceedings of the Royal Society of London. Series A, Mathematical and Physical Sciences* 195(1043):463-473. Retrieved from http://www.jstor.org/discover/10.2307/98235?uid=3739840&uid=2&uid=4&uid=3739256&sid=21102795994961

11) Vogtmann, Dana. 2009. "Stress Relaxation in Poly(methyl methacrylate) (PMMA) During Large-Strain Compression Testing Near the Glass Transition Temperature." Thesis, Department of Mechanical and Aerospace Engineering, Ohio State University, Columbus.

12) Y Luo, M Xu, X D Wang and C Liu. 2006. "Finte Element Analysis of PMMA Microfluidic Chip Based on Hot Embossing Technique." Journal of Physics: Conference Series 48(1):1102–1106. doi:10.1088/1742-6596/48/1/205.

Appendix A

x-axis: Time(ms), y-axis: True Stress (MPa)

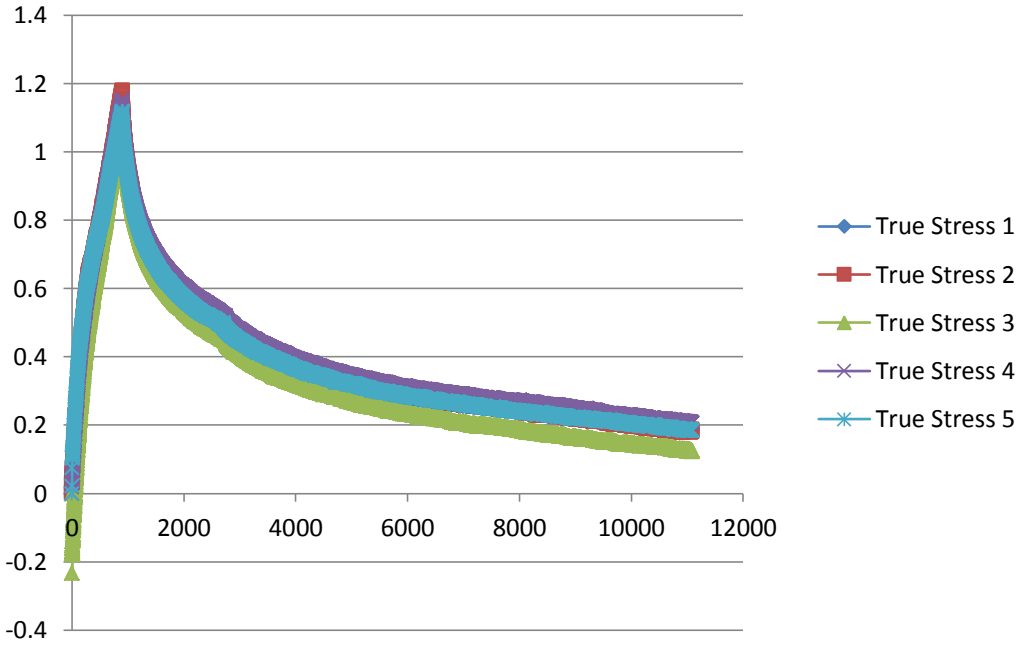

Figure 40: Samples tested at 135°C, 1/min and a total strain of 1.5

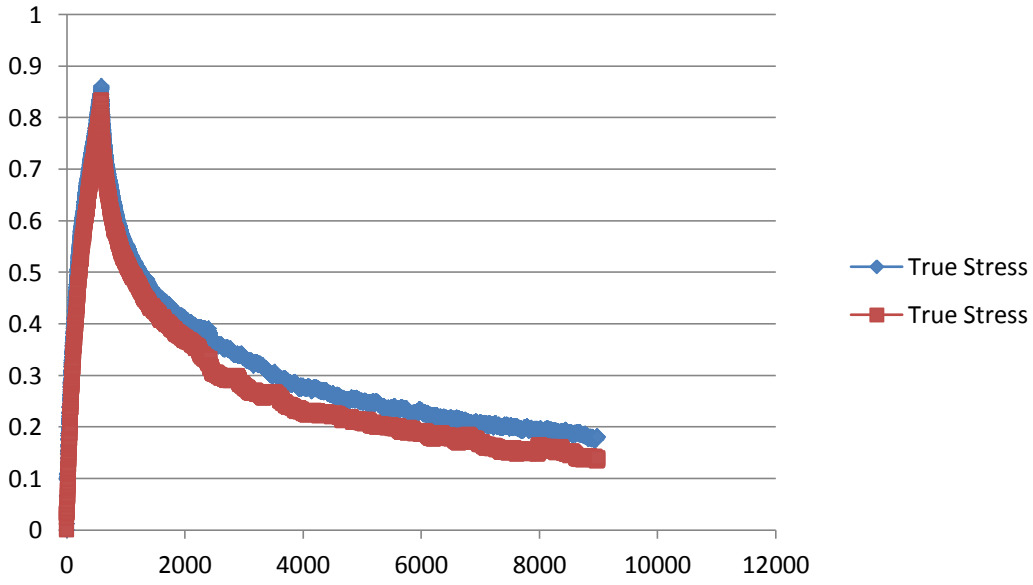

Figure 41: Samples tested at 135°C, 1/min and a total strain of 1.0

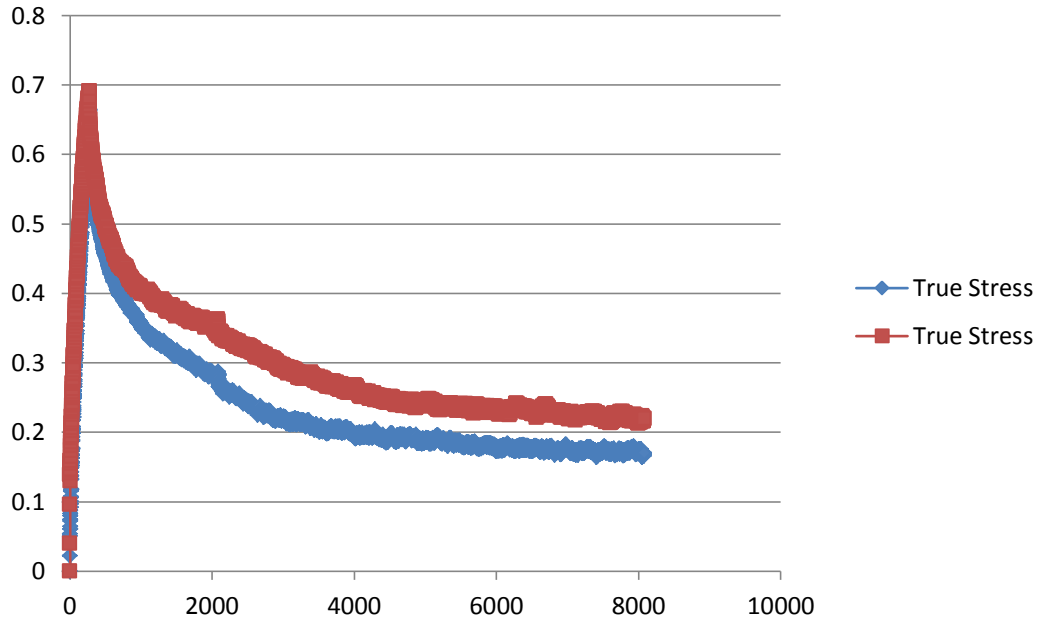

Figure 42: Samples tested at 135°C, 1/min and a total strain of 0.5

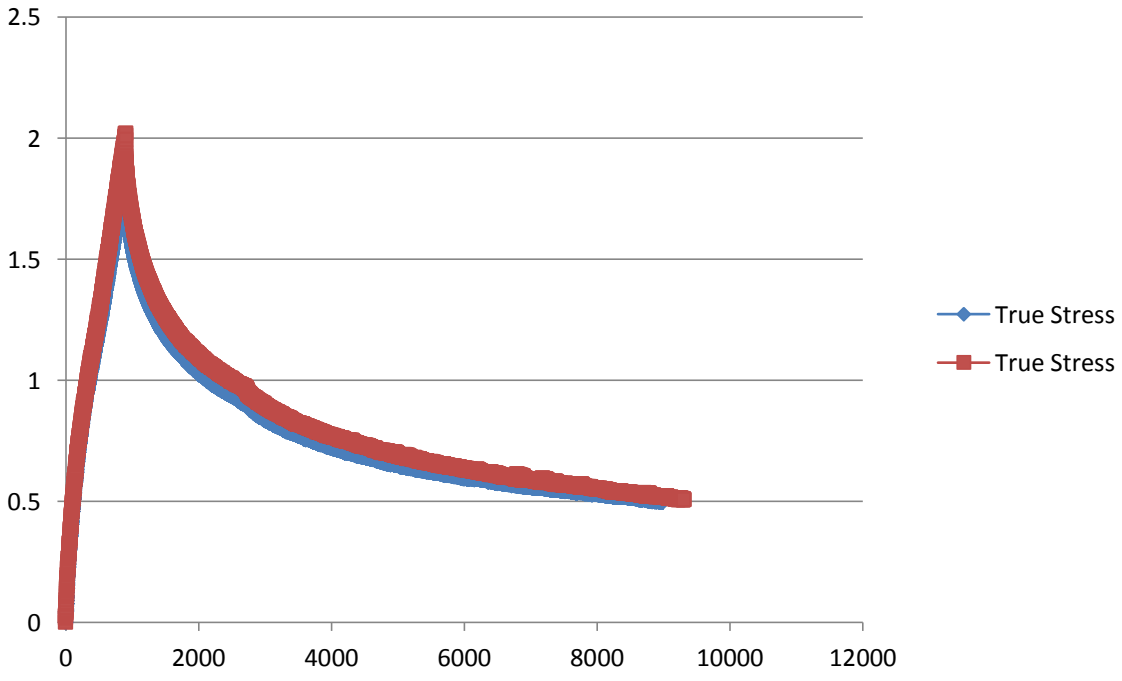

Figure 43: Samples tested at 125°C, 1/min and a total strain of 1.5

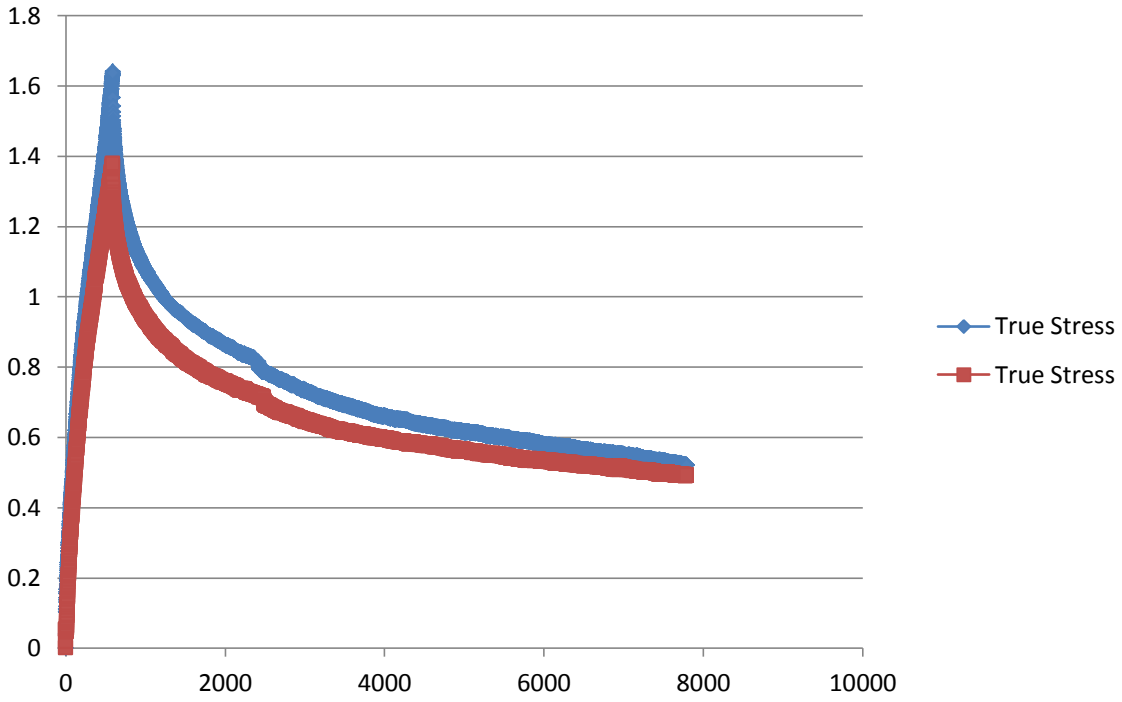

Figure 44: Samples tested at 125°C, 1/min and a total strain of 1.0

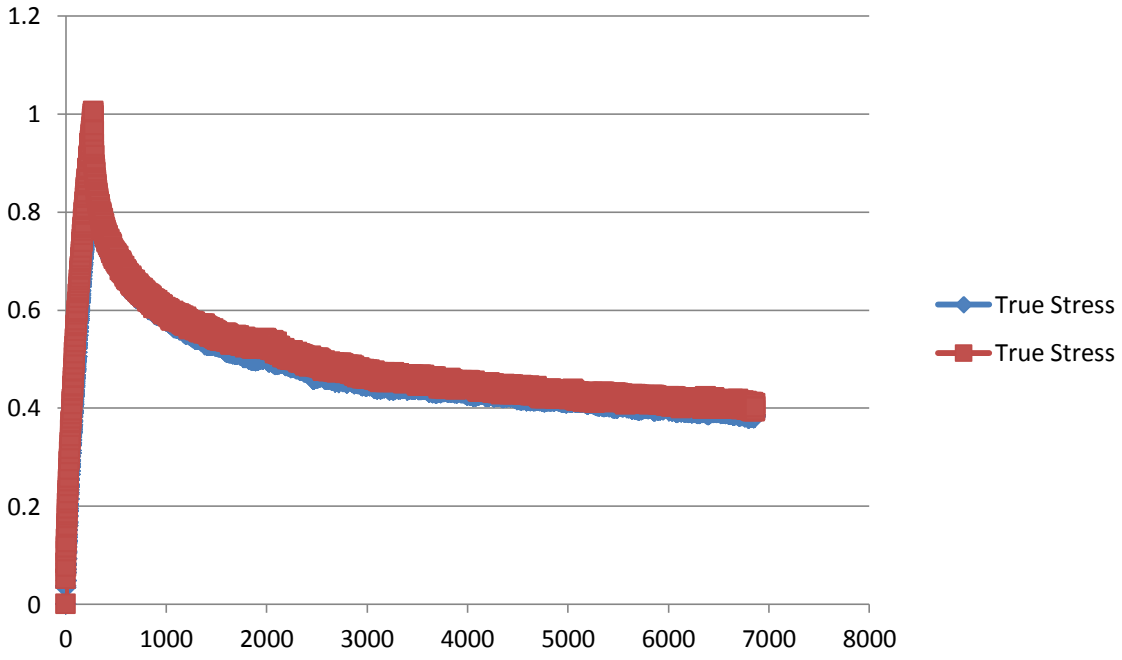

Figure 45: Samples tested at 125°C, 1/min and a total strain of 0.5

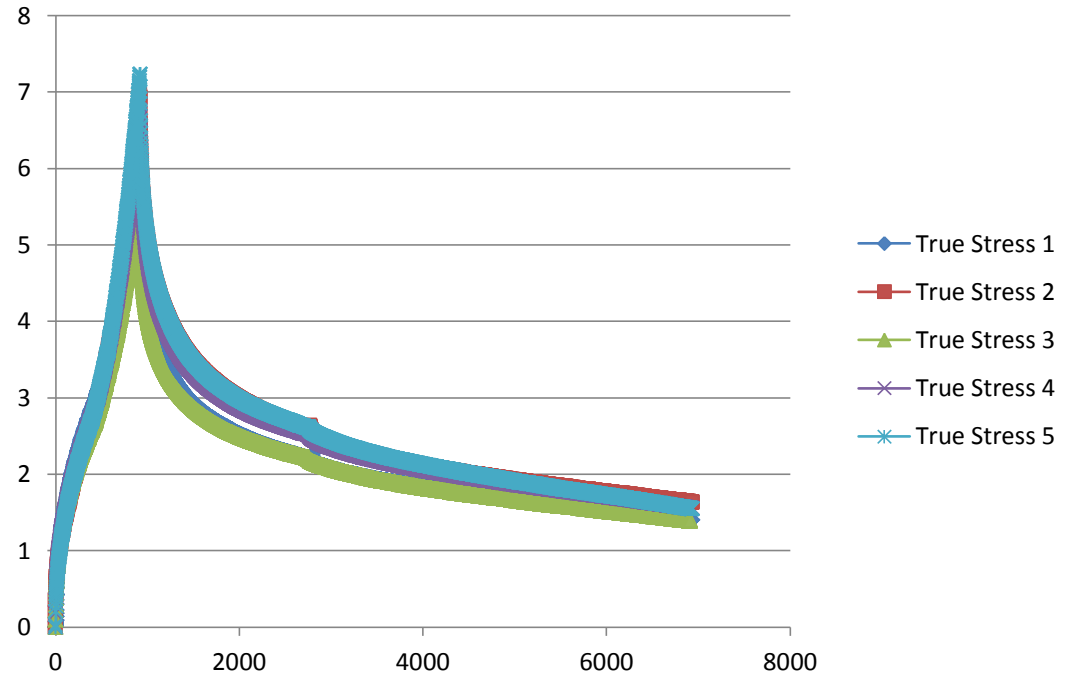

Figure 46: Samples tested at 115°C, 1/min and a total strain of 1.5

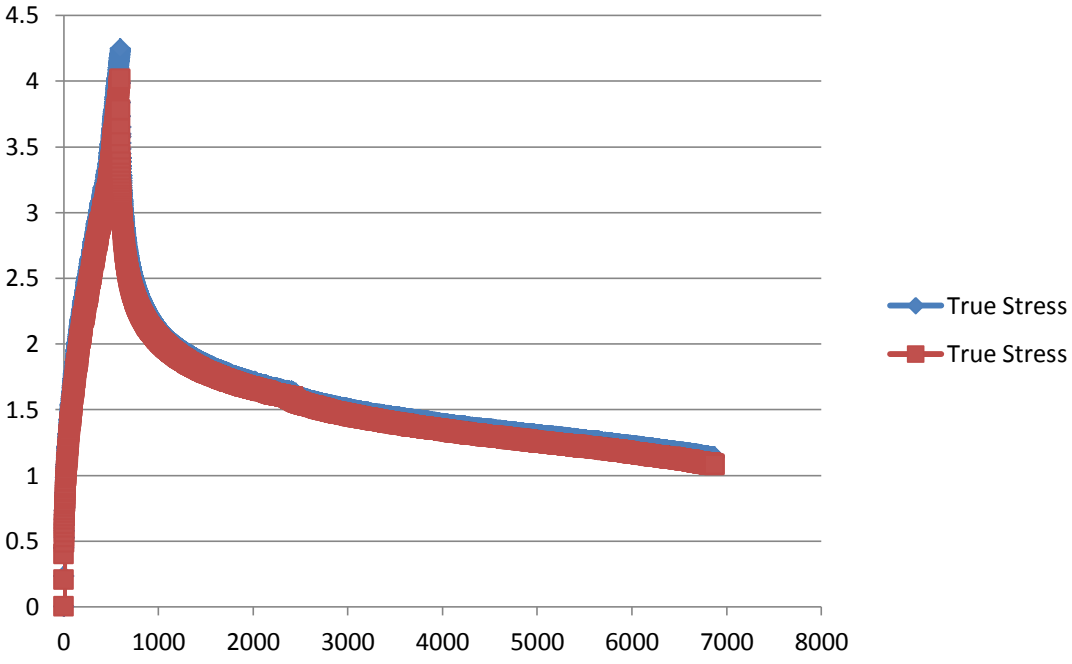

Figure 47: Samples tested at 115°C, 1/min and a total strain of 1.0

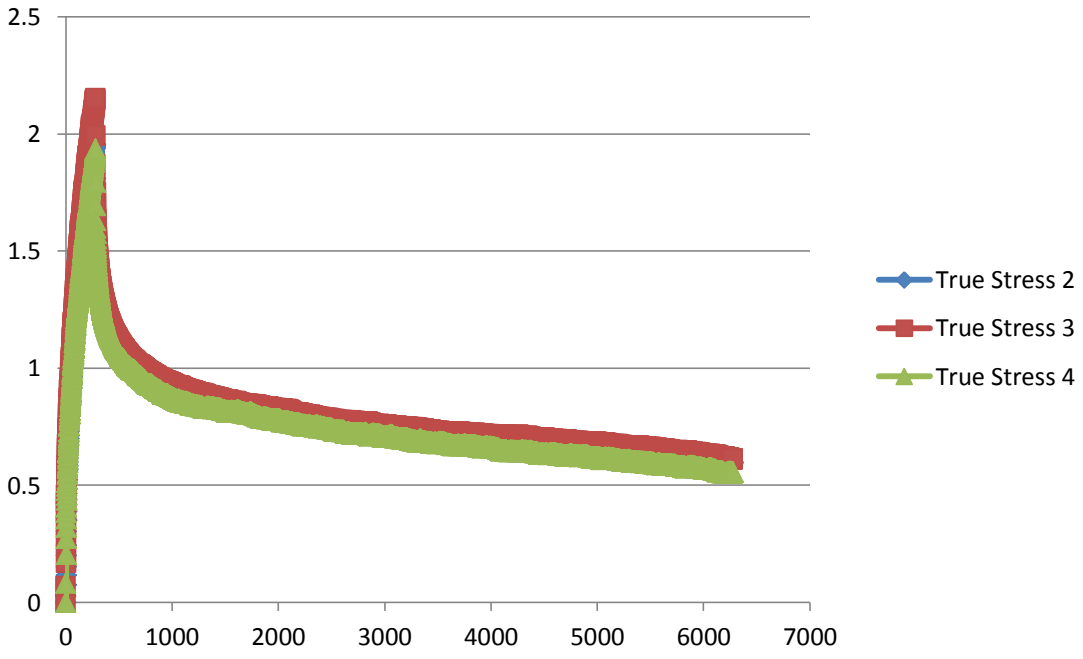

Figure 48: Samples tested at 115°C, 1/min and a total strain of 0.5

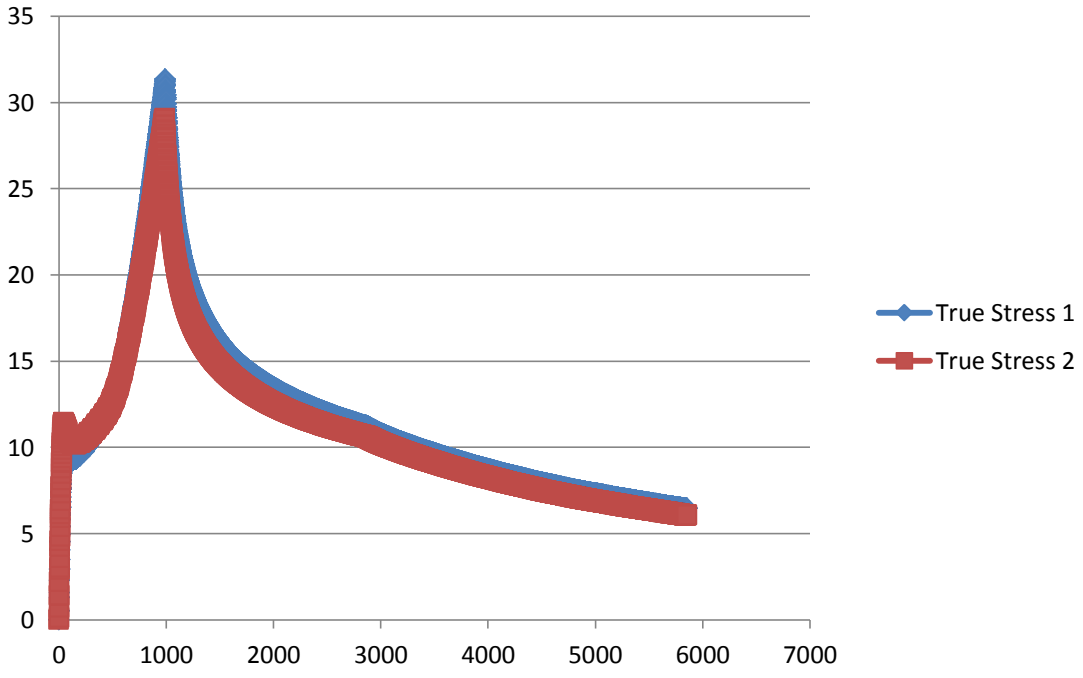

Figure 49: Samples tested at 105°C, 1/min and a total strain of 1.5

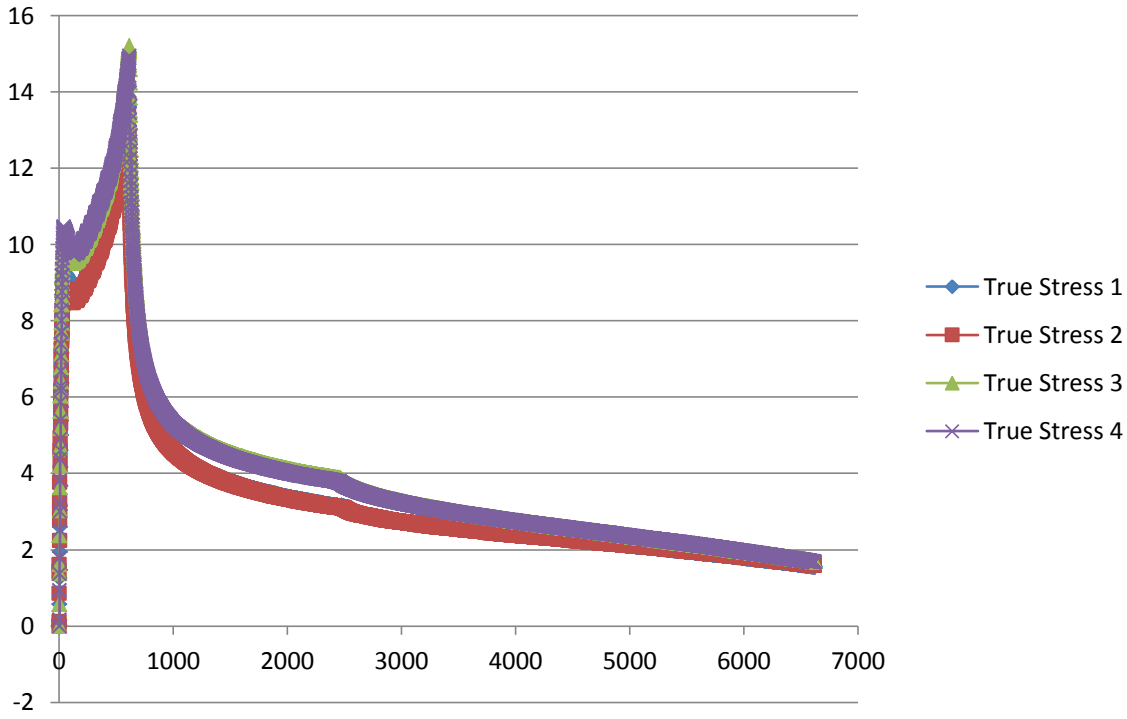

Figure 50: Samples tested at 105°C, 1/min and a total strain of 1.0

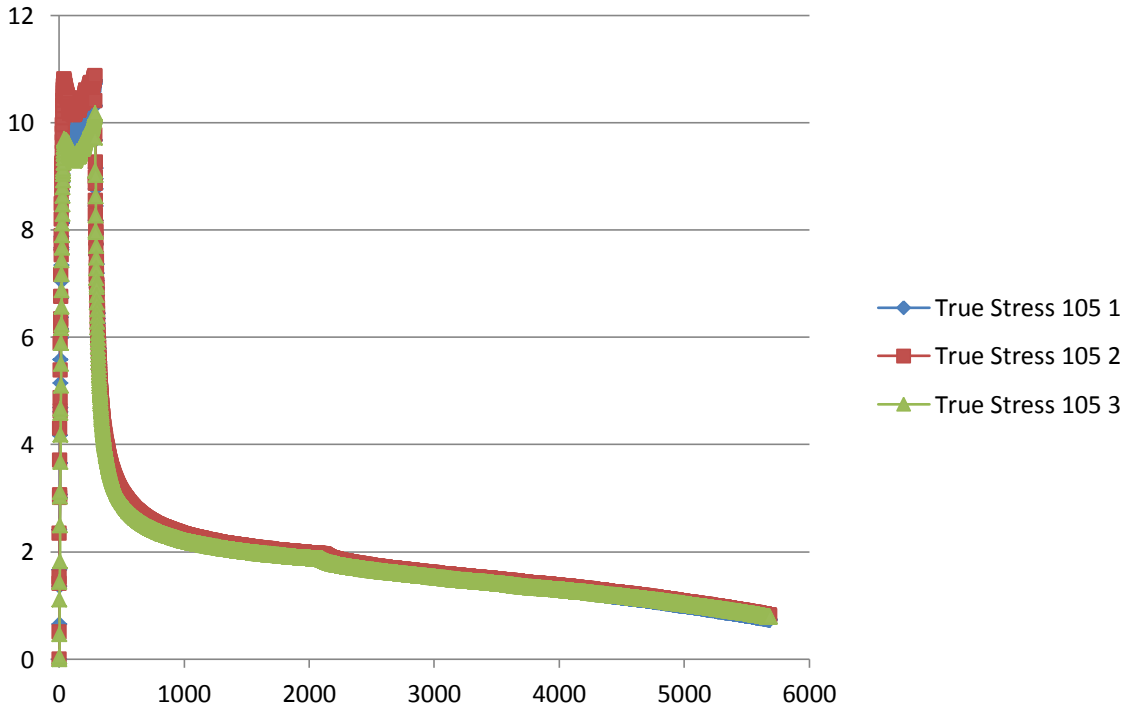

Figure 51: Samples tested at 105°C, 1/min and a total strain of 0.5

Appendix B

x-axis: Time(ms), y-axis: True Stress (MPa)

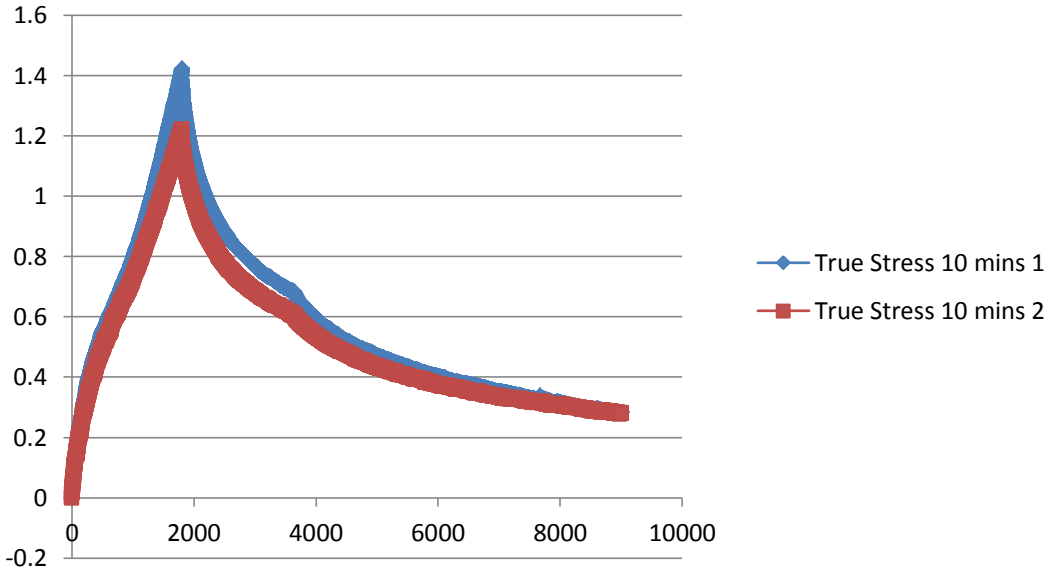

Figure 52: Samples tested at 135°C, 0.5/min and a total strain of 1.5

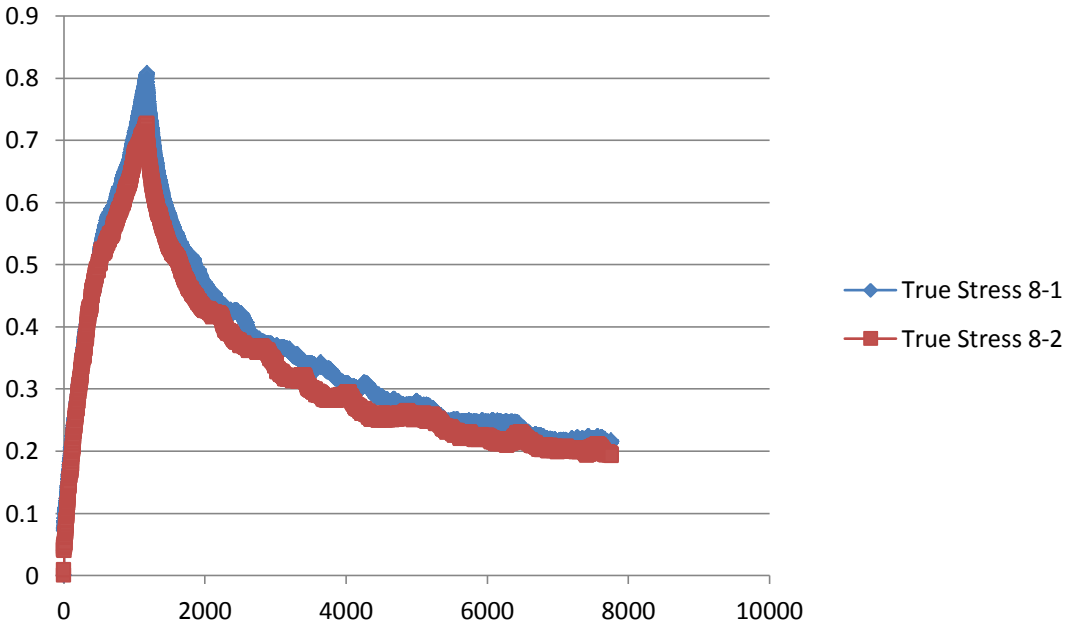

Figure 53: Samples tested at 135°C, 0.5/min and a total strain of 1.0

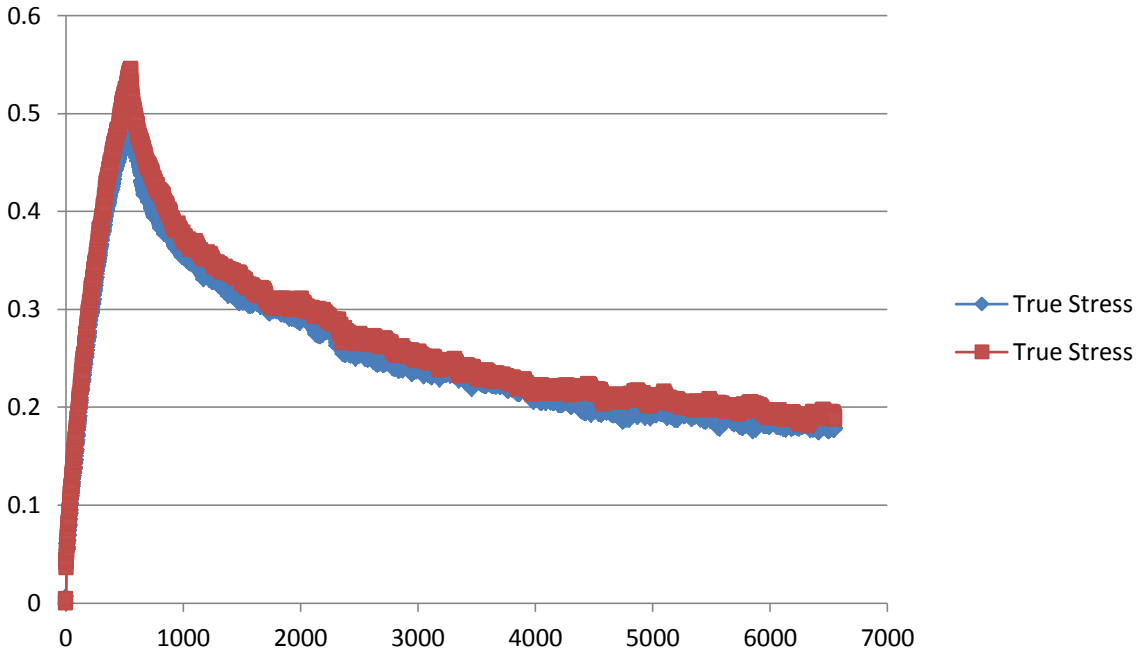

Figure 54: Samples tested at 135°C, 0.5/min and a total strain of 0.5

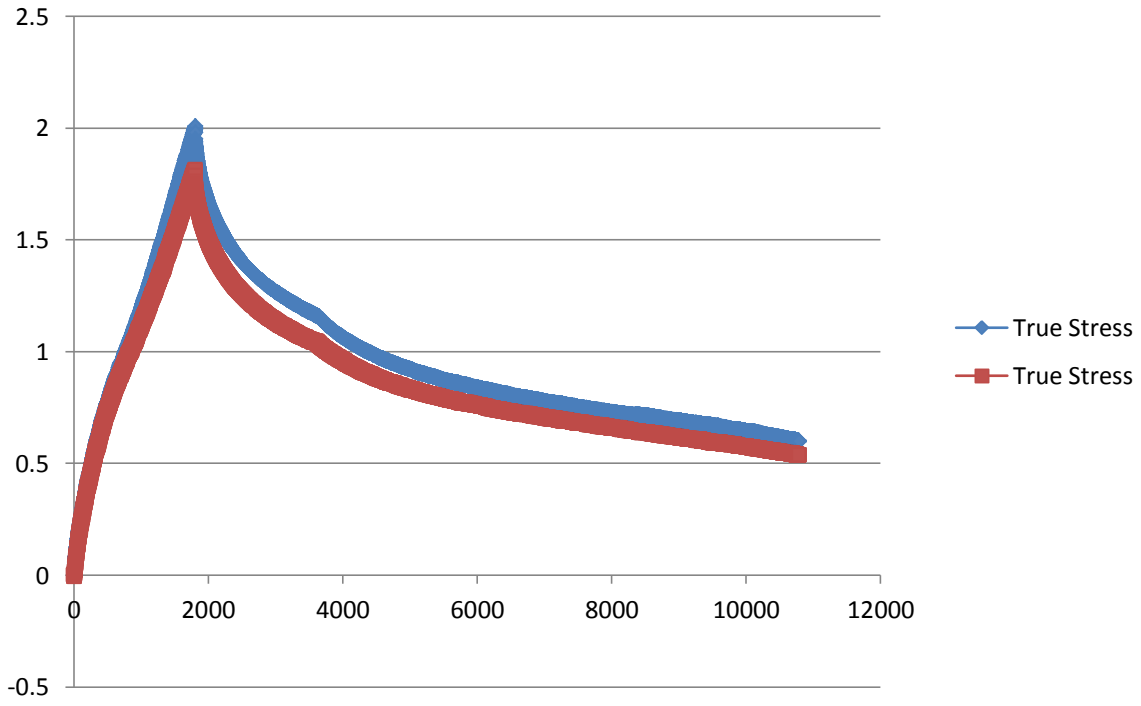

Figure 55: Samples tested at 125°C, 0.5/min and a total strain of 1.5

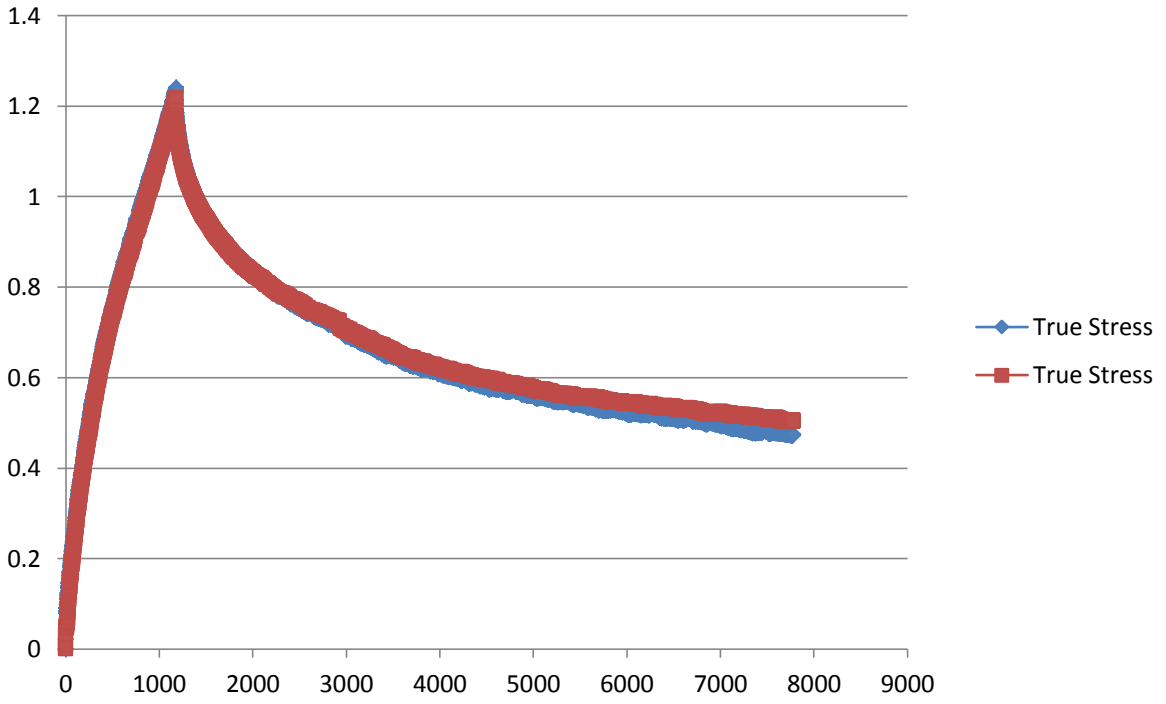

Figure 56: Samples tested at 125°C, 0.5/min and a total strain of 1.0

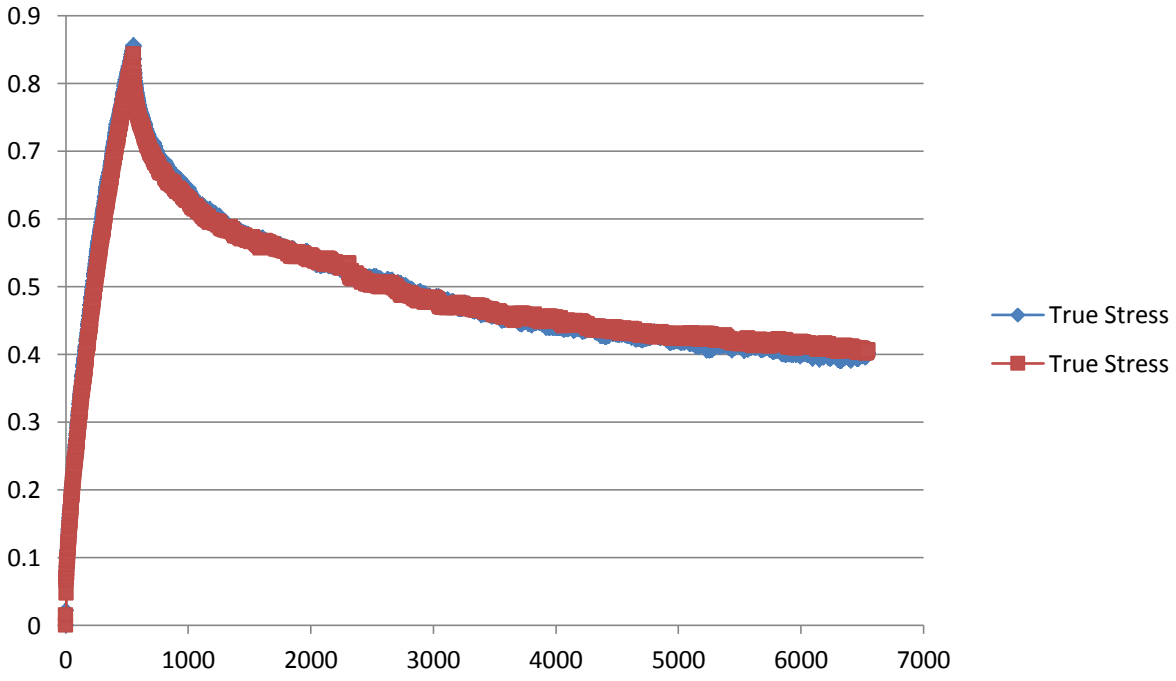

Figure 57: Samples tested at 125°C, 0.5/min and a total strain of 0.5

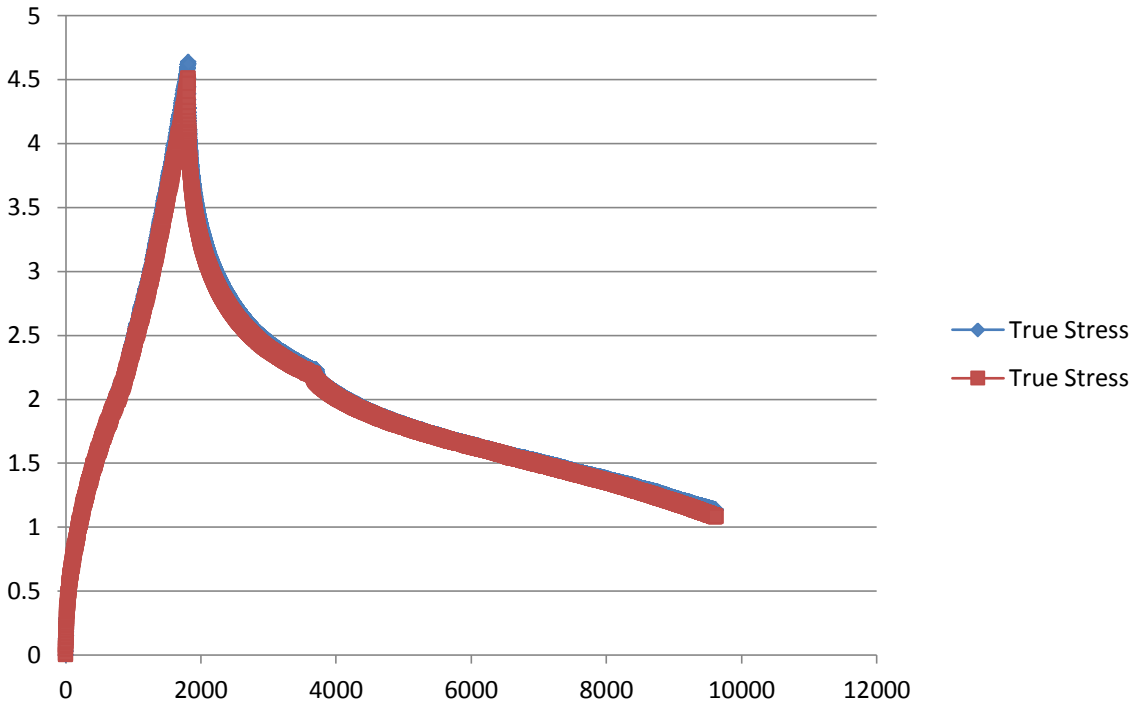

Figure 58: Samples tested at 115°C, 0.5/min and a total strain of 1.5

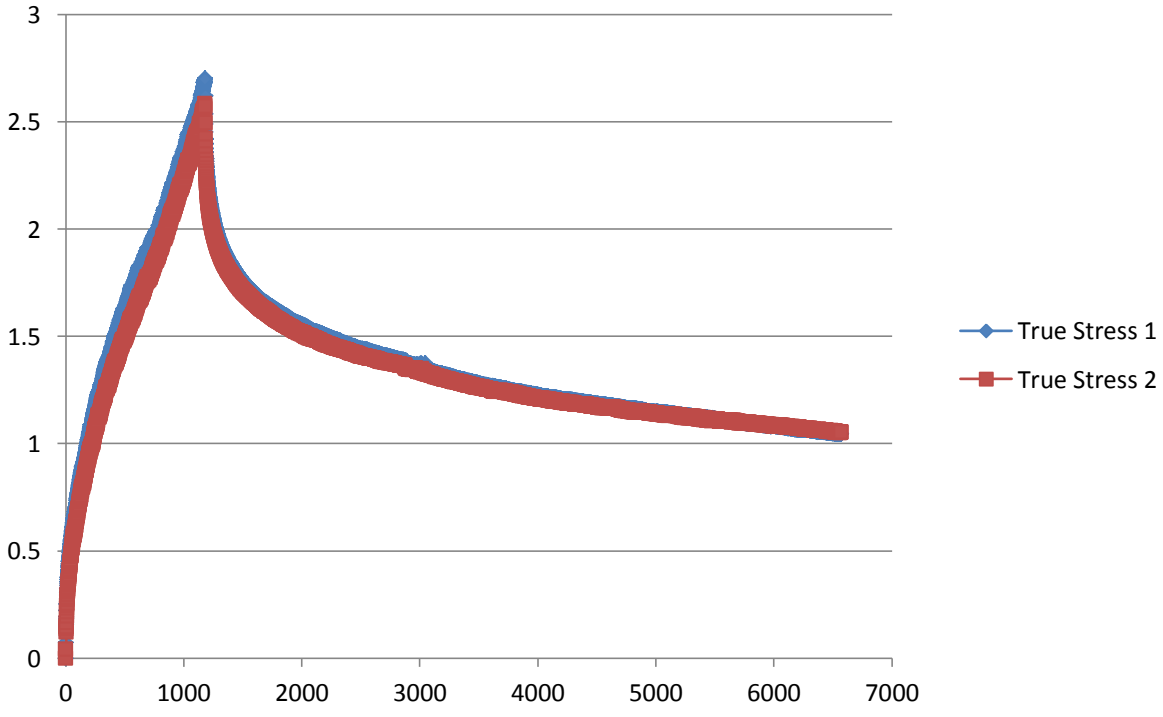

Figure 59: Samples tested at 115°C, 0.5/min and a total strain of 1.0

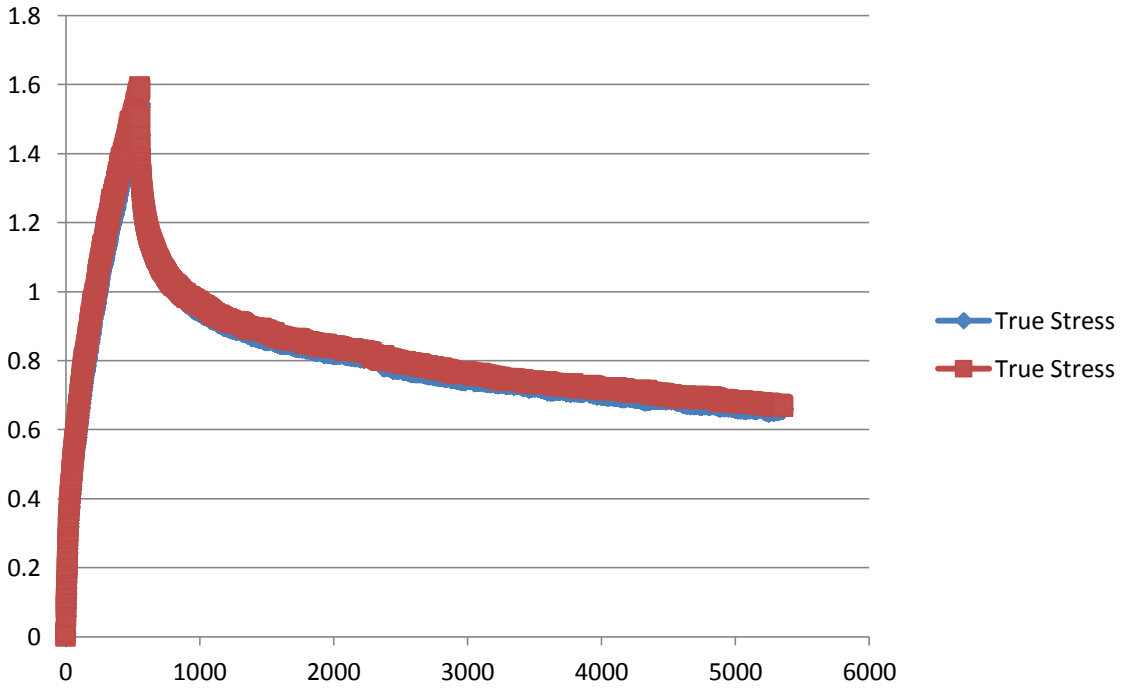

Figure 60: Samples tested at 115°C, 0.5/min and a total strain of 0.5

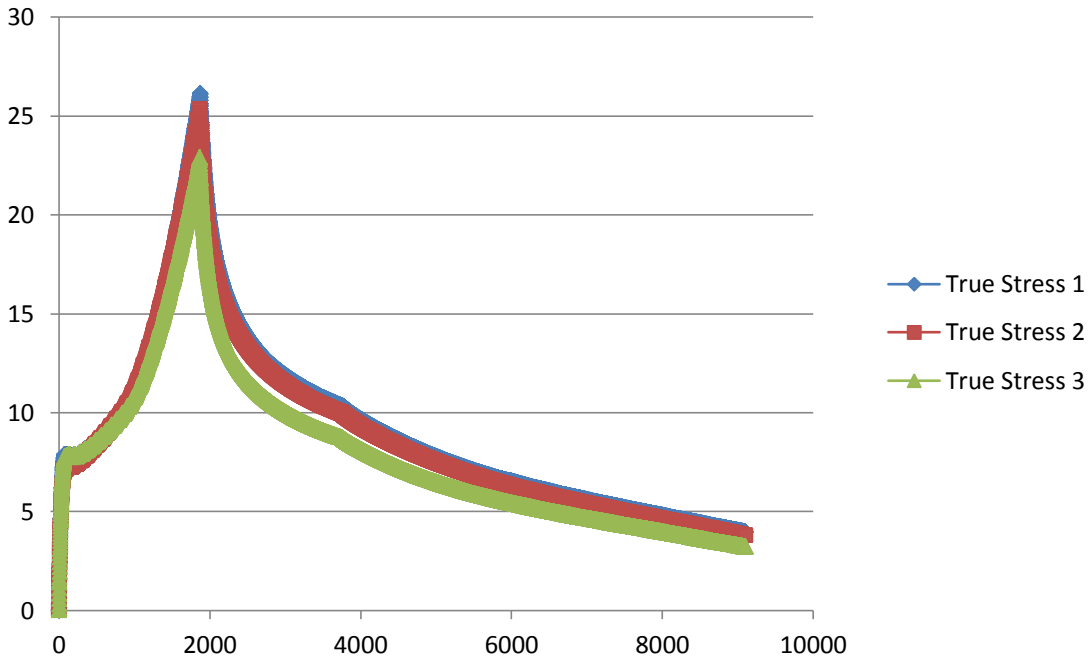

Figure 61: Samples tested at 105°C, 0.5/min and a total strain of 1.5

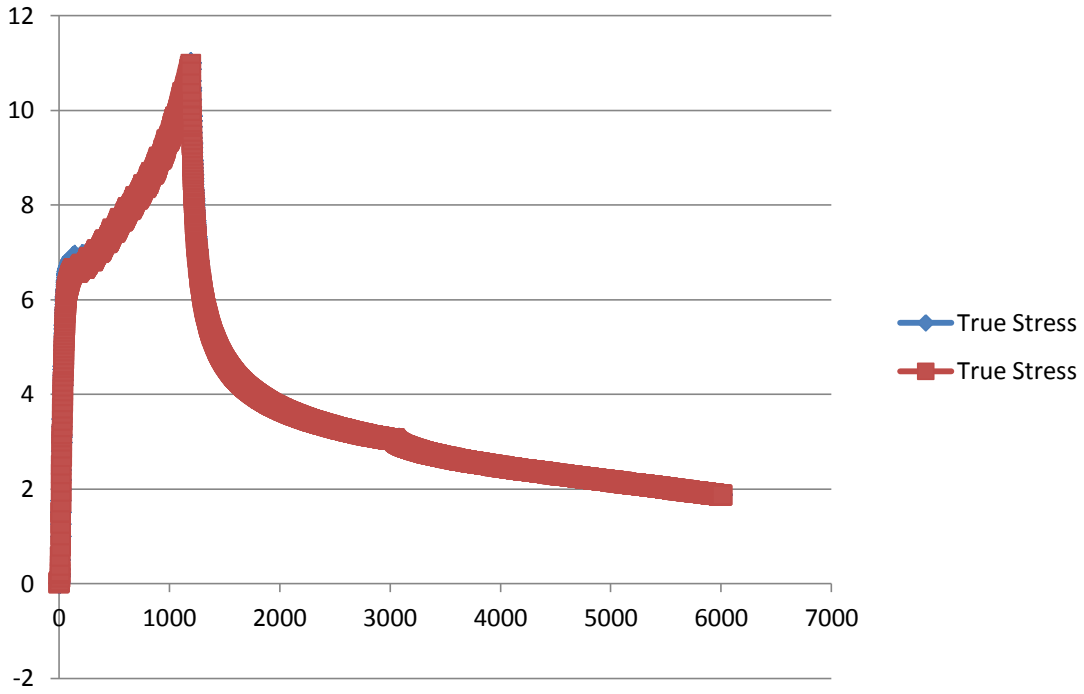

Figure 62: Samples tested at 105°C, 0.5/min and a total strain of 1.0

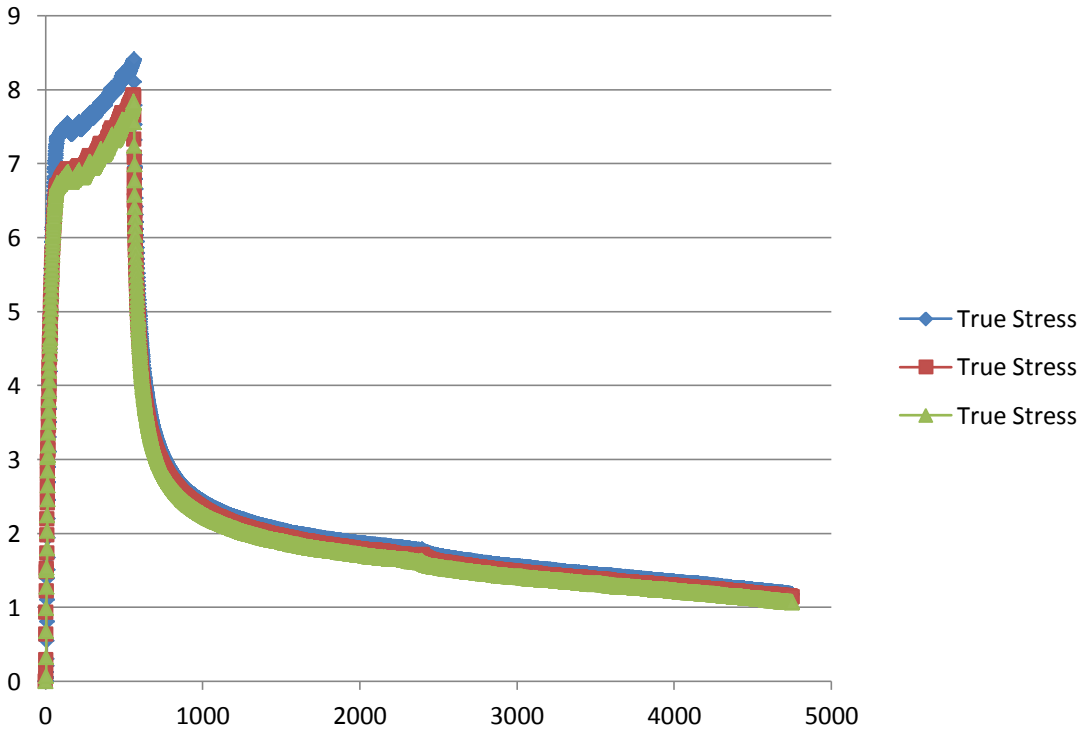

Figure 63: Samples tested at 105°C, 0.5/min and a total strain of 0.5